Therapy of Peritoneally Disseminated Colon Cancer by TAP-Deficient Embryonic Stem Cell–Derived Macrophages in Allogeneic Recipients

Eriko Haga,*,† Yuko Endo,*,† Miwa Haruta,*,† Chihiro Koba,*,† Keiko Matsumura,*,† Koutaro Takamatsu,*,† Tokunori Ikeda,*,† Yasuharu Nishimura,* and Satoru Senju*,†

We established a method to generate a large quantity of myeloid lineage cells from mouse embryonic stem (ES) cells, termed ES cell–derived proliferating myeloid cell lines (ES-ML). ES-ML continuously proliferated in the presence of M-CSF and GM-CSF. ES-ML genetically modified to express an anti-HER2 (neu) mAb single-chain V region fragment reduced the number of cocultured mouse Colon-26 cancer cells expressing HER2. Stimulation of ES-ML with IFN-γ plus LPS or TNF resulted in almost complete killing of the Colon-26 cells by the ES-ML, and the cytotoxicity was mediated, in part, by NO produced by ES-ML. When ES-ML were injected into mice with i.p. established Colon-26 tumors, they efficiently infiltrated the tumor tissues. Injection of ES-ML with rIFN-γ and LPS inhibited cancer progression in the mouse peritoneal cavity. Coinjection of TNF-transfected or untransfected ES-ML with rIFN-γ inhibited cancer growth and resulted in prolonged survival of the treated mice. In this experiment, transporter associated with Ag processing (TAP)1-deficient ES-ML exhibited therapeutic activity in MHC-mismatched allogeneic recipient mice. Despite the proliferative capacity of ES-ML, malignancy never developed from the transferred ES-ML in the recipient mice. In summary, TAP-deficient ES-ML with anticancer properties exhibited a therapeutic effect in allogeneic recipients, suggesting the possible use of TAP-deficient human-induced pluripotent stem cell–derived proliferating myeloid cell lines in cancer therapy. *The Journal of Immunology*, **2014, 193: 2024–2033.**

Macrophages reside in every tissue of the mammalian body and are engaged in various functions, such as eliminating invading pathogens, remodeling tissues, and clearing dead cells. Macrophages also infiltrate various types of cancers (1–3). Many studies indicated that tumor-associated macrophages are alternatively activated and promote cancer progression by accelerating the local invasion and metastasis of cancers (4–7). In contrast, other studies revealed the anticancer activity of macrophages in mouse or rat models (8–16). Some of these studies demonstrated the requirement for macrophages in T cell–dependent tumor rejection (11). Inoculation of TNF, PEDF, agonistic anti-CD40 mAb, CpG, or polyinosinic-polycytidylic acid into tumor-bearing mice stimulated tumor-infiltrating macrophages to kill cancer cells (12–16). These contrary observations may be due to the fact that macrophage functions are significantly affected by cytokines (17, 18).

Based on the anticancer effects of macrophages observed in preclinical studies, there have been attempts to apply macrophages to cancer therapy. For example, administration of autologous macrophages preactivated with IFN-γ to cancer patients has been tried (19–25). In the reported clinical trials, macrophages used for anticancer therapies were generated from donor peripheral blood monocytes isolated by leukapheresis. However, peripheral blood monocytes do not readily propagate; thus, the quantity, as well as the anticancer efficacy, of macrophages generated by such methods may have been insufficient to achieve therapeutic effects.

Pluripotent stem cells, such as embryonic stem (ES) cells or induced pluripotent stem (iPS) cells, can propagate indefinitely and differentiate into various types of somatic cells, including blood cells (26). Several groups, including ours, established methods to generate macrophages from mouse and human pluripotent stem cells (27–30).

In the current study, we found that introduction of the cMYC gene into mouse ES cell–derived myeloid cells (ES-MC) enabled continuous proliferation of the cells in an M-CSF– and GM-CSF–dependent manner. This procedure resulted in the generation of ES cell–derived proliferating myeloid cell lines (ES-ML), enabling us to generate a large quantity of functional macrophages. We investigated whether ES-ML with an anticancer property could exert a therapeutic effect in a mouse model of peritoneally disseminated colon cancer. In addition, we evaluated a strategy to overcome histoincompatibility between ES-ML and recipients using ES-ML deficient for transporter associated with Ag processing (TAP).

*Department of Immunogenetics, Graduate School of Medical Sciences, Kumamoto University, Kumamoto 860–8556, Japan; and †Core Research for Evolutional Science and Technology, Japan Science and Technology Agency, Kawaguchi 332–0012, Japan

Received for publication December 31, 2013. Accepted for publication June 13, 2014.

This work was supported in part by Japan Society for the Promotion of Science KAKENHI Grants 23650609, 23659158, and 24300334, Ministry of Education, Culture, Sports, Science and Technology KAKENHI Grants 22133005 and 26290057, a research grant for Intractable Diseases from the Ministry of Health and Welfare, Japan, and a grant from the Japan Science and Technology Agency.

Address correspondence and reprint requests to Dr. Satoru Senju, Department of Immunogenetics, Graduate School of Medical Sciences, Kumamoto University, Chuou-Ku, Honjo 1-1-1, Kumamoto 860-8556, Japan. E-mail address: senjusat@gpo.kumamoto-u.ac.jp

The online version of this article contains supplemental material.

Abbreviations used in this article: CBF1, (BALB/c × C57BL/6) F1; Colon/HL, HER2 and firefly luciferase–expressing Colon-26 mouse adenocarcinoma cells; ES, embryonic stem; ES-MC, ES cell–derived myeloid cell; ES-ML, ES cell–derived proliferating myeloid cell line; ES-ML/anti-HER2, ES-ML expressing an anti-HER2 single chain V region fragment; ES-ML/TNF, TNF-transfectant ES-ML; iPS, induced pluripotent stem; iPS-ML, iPS cell–derived proliferating myeloid cell line; IRES, internal ribosomal entry site; scFv, single chain V region fragment; TAP, transporter associated with Ag processing; tPA, tissue plasminogen activator.

www.jimmunol.org/cgi/doi/10.4049/jimmunol.1303473

Materials and Methods

Mice

Mouse experiments were performed under the approval of the Animal Research Committee of Kumamoto University. Six- to eight-wk-old BALB/c or (BALB/c × C57BL/6) F1 (CBF1) mice were purchased from Japan SLC (Hamamatsu, Japan) and housed under specific pathogen–free conditions at the Center for Animal Resources and Development (Kumamoto University).

Flow cytometric analysis

The following mAb conjugated with FITC or PE were purchased from BD Pharmingen (San Diego, CA), Miltenyi Biotec (Bergisch Gladbach, Germany), or eBioscience (San Diego, CA): anti-CD45 (clone 30-F11), anti-CD11b (clone M1/70), anti-CD14 (clone Sa2-8), anti-F4/80 (clone BM8), anti-HER2/neu (clone Neu 24.7), anti-cMYC (clone SH1-26E7.1.3.), and anti–H2-K^b (AF6-88.5.5.3). Polyclonal goat anti-mouse TNFRI and II Ab, polyclonal goat IgG (R&D Systems, Minneapolis, MN), and FITC-conjugated rabbit anti-goat IgG Ab (Sigma-Aldrich, St. Louis, MO) also were used. Cells were stained with the fluorochrome-conjugated mAb for 40 min and then washed twice with PBS containing 2% FCS. Stained cells were analyzed on a FACScan or FACSCalibur flow cytometer (Becton Dickinson).

Generation of ES-ML

ES cells derived from the C57BL/6 strain were kindly provided by Drs. N. Nakatsuji and H. Suemori (Kyoto University, Kyoto, Japan). Gene targeting of the TAP1 gene in E14 ES cells derived from the 129/sv strain (H-2^b) to generate TAP1$^{-/-}$ ES cells was performed as reported previously (31). Differentiation of ES cells to generate ES-MC was performed as described previously (32). The human cMYC gene was introduced into ES-MC, prepared from the second step of the differentiation culture, using a lentiviral vector to establish a proliferating myeloid cell line (ES-ML). ES-ML were maintained in RPMI 1640 medium containing 10% FCS, mouse GM-CSF (10–20 ng/ml), and human M-CSF (20–50 ng/ml).

Construction of HER2 and anti-HER2 mAb expression vectors

cDNA for mAb single chain V region fragment (scFv) specific to HER2 (neu) was a gift from Dr. J. Lieberman (Addgene plasmid #10794, Harvard Medical School, Boston, MA) (33). The scFv sequence was linked by PCR with DNA encoding a cMYC tag (EQKLISEEDL) and a C-terminal

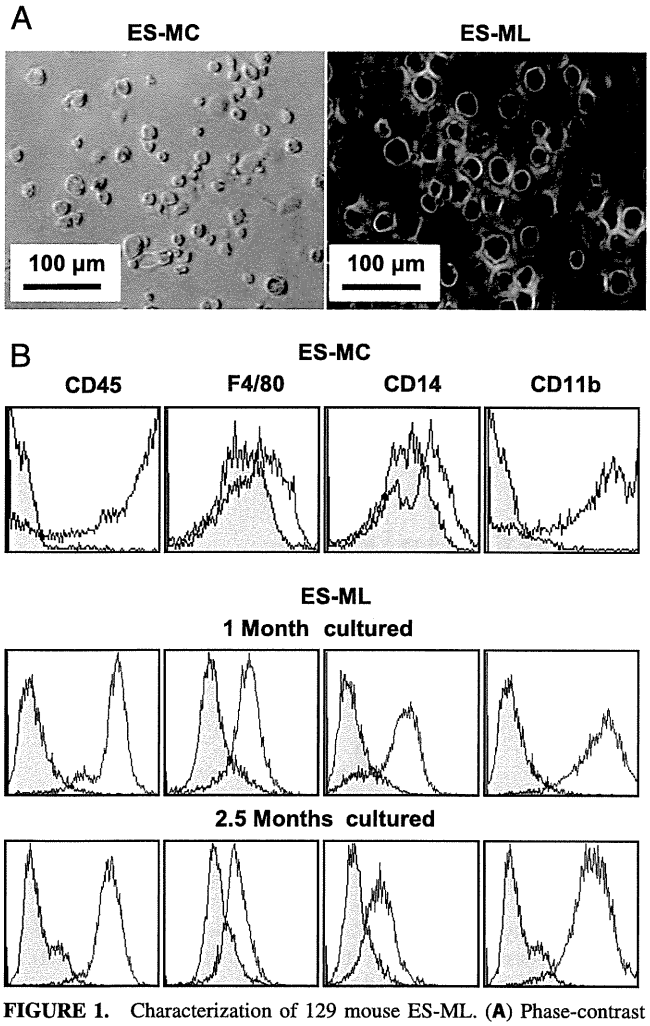

FIGURE 1. Characterization of 129 mouse ES-ML. (**A**) Phase-contrast images of ES-MC and ES-ML. (**B**) Flow cytometric analysis of CD45, CD11b, F4/80, and CD14 on ES-MC and ES-ML. ES-MC were generated by differentiation culture established previously (32). ES-ML cultured for 1 or 2.5 mo after introduction of c-Myc were analyzed. The staining profiles of specific mAbs (open graph) and isotype-matched control mAbs (shaded graph) are shown.

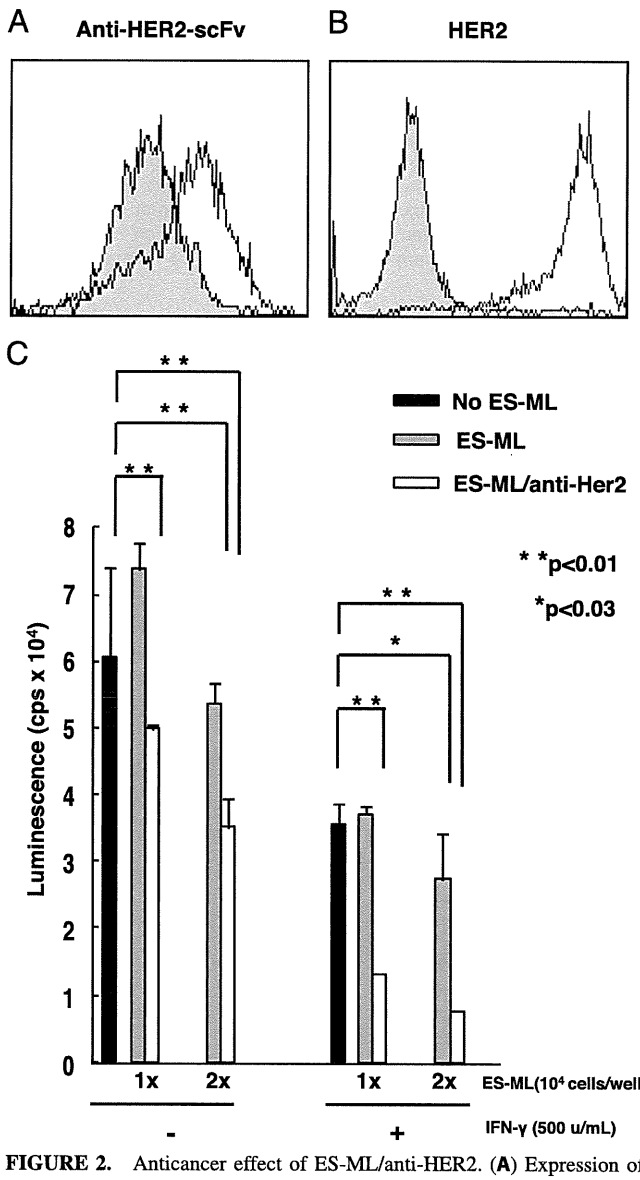

FIGURE 2. Anticancer effect of ES-ML/anti-HER2. (**A**) Expression of an anti-HER2 scFv in ES-ML/anti-HER2 was analyzed by staining with an anti-cMYC tag mAb. The staining profiles of the anti-cMYC tag mAb (open graph) and isotype-matched control mAb (shaded graph) are shown. (**B**) Expression of HER2 in HER2 and firefly luciferase–expressing Colon-26 mouse adenocarcinoma cells (Colon/HL). (**C**) Colon/HL (5×10^3 cells/well) were cultured alone (black bars) or cocultured with 1 or 2×10^4 ES-ML (gray bars) or ES-ML/anti-HER2 (white bars) in the presence or absence of IFN-γ (500 U/ml) in a 96-well culture plate. After 3 d of culture, the number of live Colon/HL was measured by luciferase activity. Data are mean luminescence counts per second (cps) + SD of duplicate assays.

fragment of mouse FcγRI. cDNA for HER2 was obtained from the human breast cancer cell line MCF7. The cDNA were cloned into the mammalian expression vector pCAG- internal ribosomal entry site (IRES)-puroR driven by the CAG promoter and including an IRES-puromycin *N*-acetyl-transferase gene cassette.

Generation of lentiviral vectors

cDNA of human cMYC and mouse TNF were obtained by PCR and cloned into a pENTR-TOPO vector (Invitrogen, Carlsbad, CA). The cDNA fragments were inserted into the lentiviral vector CSII-EF (34) (a gift from Dr. H. Miyoshi together with the packaging constructs, RIKEN, Tsukuba, Japan), with or without IRES-puroR, to generate lentiviral expression constructs. Recombinant lentivirus was produced and purified by a previously described method (28).

Analysis of the antitumor activity of ES-ML in vitro

Colon-26 mouse adenocarcinoma cells, provided by RIKEN, were transfected with expression vectors for HER2 and firefly luciferase by electroporation to generate HER2 and firefly luciferase–expressing Colon-26 mouse adenocarcinoma cells (Colon/HL). Colon/HL (2.5–5 × 10^3 cells/well) were cultured with the indicated numbers of ES-ML in the presence of IFN-γ (PeproTech, Rocky Hill, NJ), LPS (Sigma-Aldrich), mouse TNF (PeproTech), L-NAME (Dojindo, Kumamoto, Japan), L-NMMA (Dojindo), or NOR-5 (Dojindo) in 96-well flat-bottom culture plates (B&W Isoplate; PerkinElmer, Waltham, MA). After 3 d of culture, 50 μl luciferase substrate solution (steadylite plus; PerkinElmer) was added to each well, and the luminescence was measured by a microplate reader (TriStar; Berthold Technologies, Bad Wildbad, Germany). In some experiments, ES-ML were pretreated with IFN-γ (200 U/ml), IFN-γ plus LPS (0.03 μg/ml), or IFN-γ plus TNF (10 ng/ml) for 24 h, harvested, and washed. The pretreated or untreated ES-ML (1 × 10^4 cells/well) were cocultured with Colon/HL (2.5 × 10^3 cells/well). Production of NO in ES-ML was quantified by determining the concentration of NO_2 + NO_3 in culture supernatants by the Griess method using a NO assay kit (Dojindo).

Analysis of ES-ML cell infiltration into cancer tissues

Colon-26 cells (2 × 10^6 cells/mouse) were injected into the peritoneal cavity of BALB/c mice. After 7 d, ES-ML labeled with PKH26 (Sigma-Aldrich) were injected i.p. into the mice (5 × 10^7 cells/mouse), with or without tissue plasminogen activator (tPA; 5000 U/mouse; Technoclone, Vienna, Austria). Mice were sacrificed on the next day, and cancer tissues in the greater omentum and mesenterium were removed, fixed in 4% paraformaldehyde/PBS, and embedded in Tissue-TEK O.C.T. compound (Sakura Finetek, Tokyo, Japan). Twenty-micron-thick frozen sections were prepared on a cryostat (MICROM HN505N; Thermo Scientific, Kalamazoo, MI), nuclear stained with DAPI, and analyzed under a fluorescence microscope (Axio Observer Z1; Carl Zeiss, Oberkochen, Germany).

Analysis of the antitumor activity of ES-ML in vivo

Mice were injected i.p. with Colon/HL (1–2 × 10^6 cells/mouse). On day 2, D-Luciferin (3 mg/mouse; Advanced Assay Technologies, Sunnyvale, CA) was injected i.p. into the anesthetized mice, and luminescence images

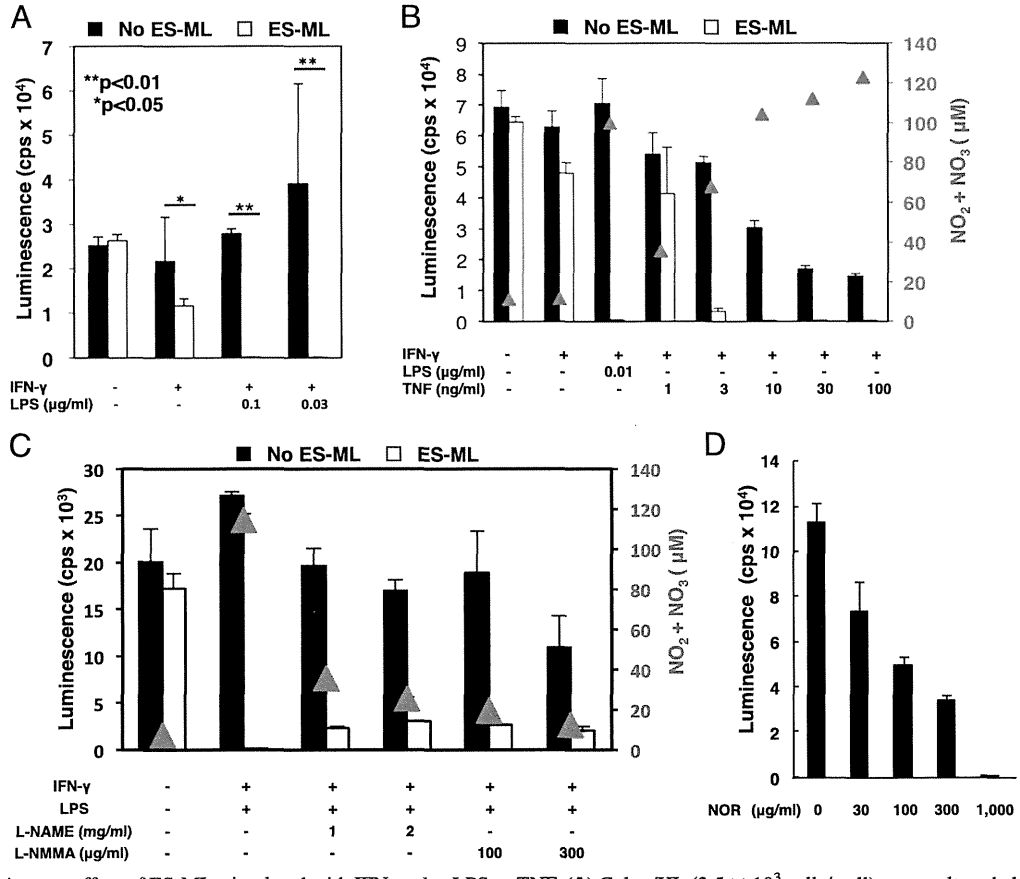

FIGURE 3. Anticancer effect of ES-ML stimulated with IFN-γ plus LPS or TNF. (**A**) Colon/HL (2.5 × 10^3 cells/well) were cultured alone (black bars) or cocultured with ES-ML/anti-HER2 (1 × 10^4 cells/well; white bars) in a 96-well culture plate in the presence or absence of IFN-γ (200 U/ml) and LPS (0.1 or 0.03 μg/ml). The number of live Colon/HL was measured on day 3 by luciferase activity. (**B**) Colon/HL (2.5 × 10^3 cells/well) were cultured alone (black bars) or cocultured with ES-ML/anti-HER2 (1 × 10^4 cells/well; white bars) in the presence or absence of IFN-γ (200 U/ml), LPS (0.01 μg/ml), or TNF (1–100 ng/ml) for 3 d. NO production from ES-ML was measured by quantifying the concentrations of NO_2 and NO_3 in the culture supernatant by the Griess method; the results are indicated by red triangles. (**C**) Colon/HL (2.5 × 10^3 cells/well) were cultured alone (black bars) or cocultured with ES-ML/anti-HER2 cells (white bars) in a 96-well culture plate in the presence or absence of IFN-γ (200 U/ml), LPS (0.1 μg/ml), L-NAME (1 or 2 mg/ml), or L-NMMA (100 or 300 μg/ml) for 3 d. Production of NO by ES-ML was measured and presented as in (B). The number of live Colon/HL was determined by luciferase activity. (**D**) Colon/HL (2.5 × 10^3 cells/well) were cultured in a 96-well culture plate in the presence or absence of NOR-5 (30–1000 μg/ml) for 24 h. The number of live Colon/HL was determined by luciferase activity. Data are the mean luminescence counts per second (cps) + SD of triplicate (A, B, and D) or duplicate (C) assays.

were obtained by an in vivo imaging system (NightOWL II; Berthold Technologies) under anesthesia with isoflurane inhalation plus tribromoethanol injection. Mice carrying established tumors were divided into therapy and control groups. Therapy group mice were administered ES-ML and IFN-γ. In some experiments, LPS, M-CSF, collagenase, and hyaluronidase also were administered, as indicated. Cancer progression was monitored by luminescence imaging analysis on days 7 and 14 and quantified by the total luminescence count for each mouse.

Statistical analysis

Student *t* test was used for the statistical analysis of data from in vitro experiments. Statistical analysis of the results from in vivo experiments was done using the Mann–Whitney *U* test or the log-rank test, as indicated. A p value < 0.05 was considered significant.

Results

Generation and characterization of mouse ES-MC with a proliferative capacity

We previously established a method to generate dendritic cells and macrophages from mouse pluripotent stem cells (23, 28). In the current study, we found that forced expression of cMYC induced proliferation of ES-MC and established the method to generate ES-ML (Fig. 1A). Both ES-MC and ES-ML expressed the panleukocyte marker CD45 and macrophage markers F4/80, CD14, and CD11b (Fig. 1B). ES-ML continuously grew in the presence of GM-CSF and M-CSF for at least several months, with a doubling time of 2–3 d. This simple technique enabled us to readily generate a large quantity of mouse myeloid cells.

Anticancer effect of ES-ML in vitro

HER2/neu is expressed in various human malignancies, including colon cancer (35, 36). A humanized Ab against HER2, trastuzumab, is widely used for the treatment of breast and gastric cancers (37, 38). Ab-dependent cellular cytotoxicity mediated by NK cells and macrophages is considered a critical mechanism underlying the effect of anticancer Ab therapies (39). We expected that ES-ML expressing an anti-HER2 scFv (ES-ML/anti-HER2) would attack cancer cells expressing HER2. To ensure that the transfectant ES-ML execute Ab-dependent cellular cytotoxicity mimicking cytotoxicity upon encounter with HER2-expressing target cells, the scFv was linked to the transmembrane and cytoplasmic domains of FcγRI. Cell surface expression of scFv fused to FcγRI was detected by staining with anti-cMYC tag mAb (Fig. 2A).

We evaluated the effect of ES-ML/anti-HER2 against cancer cells expressing HER2 in vitro. To this end, we generated Colon/HL (Fig. 2B). We established an experimental system to examine the effect of ES-ML on cocultured Colon/HL, in which the number of live Colon/HL was quantitated by luciferase activity. ES-ML/anti-HER2 showed a certain degree of activity to reduce the number of cocultured Colon/HL (Fig. 2C). Addition of IFN-γ to the culture synergistically enhanced the effect of ES-ML/anti-HER2 on Colon/HL (Fig. 2C).

We tested several factors for their ability to enhance the anticancer effect of ES-ML and found that simultaneous addition of IFN-γ plus LPS resulted in almost complete killing of Colon/HL (Fig. 3A). The disappearance of live Colon/HL induced by IFN-γ plus LPS was observed only in the presence of ES-ML (Fig. 3A). Therefore, the dramatic killing of Colon/HL was not a direct effect of IFN-γ and LPS on Colon/HL but was mediated by ES-ML stimulated with IFN-γ plus LPS. The dramatic killing of Colon/HL by ES-ML also was observed when IFN-γ plus TNF were added to the coculture (Fig. 3B). In contrast, ES-ML pretreated with IFN-γ, IFN-γ plus LPS, or IFN-γ plus TNF for 24 h did not exhibit significant killing of Colon/HL, suggesting that the anticancer effect of ES-ML induced by the factors promptly decreased after removal of the stimulating factors (Supplemental Fig. 1).

Induction of NO synthase 2 and production of NO by mouse macrophages upon stimulation with IFN-γ and LPS were reported previously (40, 41). ES-ML also produced NO when stimulated with IFN-γ plus LPS or IFN-γ plus TNF, and the magnitude of cytotoxicity was in parallel with the amount of NO produced by ES-ML (Fig. 3B). To assess the possibility that the killing of Colon/HL was mediated by NO, we added NO synthase inhibitors, L-NAME or L-NMMA (42), to the cultures. Colon/HL cell death was partly inhibited by either of these drugs (Fig. 3C), suggesting that the cytotoxicity was mediated by NO, at least in part. In addition, a NO-donor chemical (NOR-5) killed Colon/HL in

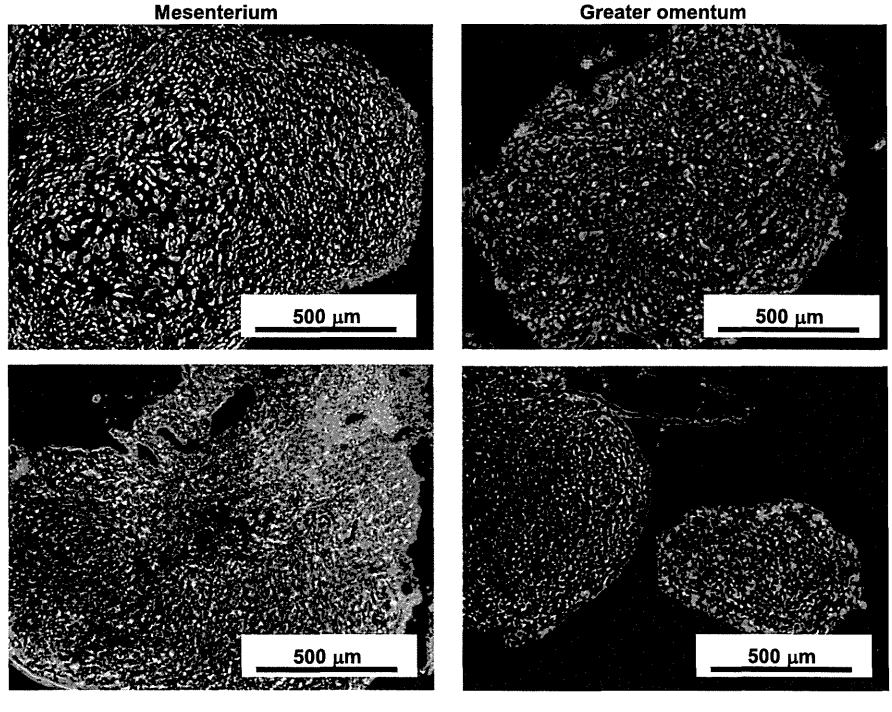

FIGURE 4. Infiltration of i.p. injected ES-ML into tumor tissues. Colon/HL (2×10^6 cells/mouse) were injected into the peritoneal cavity of mice. After 7 d, ES-ML labeled with the fluorescent dye PKH26 were injected i.p. into the mice (5×10^7 cells/mouse) with (*lower panels*) or without (*upper panels*) tPA (5000 U/mouse). The mice were sacrificed the next day, and the tumor tissues in the peritoneal cavity were isolated, fixed, and sectioned at 20-μm thicknesses. The sections were stained with DAPI and analyzed under a fluorescence microscope. Cancer tissues isolated from the mesenterium and greater omentum are shown. PKH26–labeled ES-ML were visualized by red fluorescence.

a dose-dependent manner (Fig. 3D), indicating that Colon/HL is sensitive to NO.

Infiltration of ES-ML into cancer tissues in vivo

Macrophage infiltration is frequently observed in clinical samples of cancer tissues. We examined whether exogenously administered ES-ML also infiltrated pre-established cancer tissues in vivo. We injected Colon/HL i.p. into the mice. After 7 d, we injected ES-ML labeled with the fluorescent dye PKH26. For some mice, we injected tPA simultaneously with ES-ML, intending to enhance the tissue infiltration of ES-ML. The next day, the mice were sacrificed, and the tumor masses in the greater omentum and mesenterium were collected for microscopic examination.

Fig. 4 shows the fluorescence images of the tumor tissue sections. We observed infiltrating ES-ML in the cancer tissues, indicating migration of ES-ML directed to tumor tissues. Coinjection with tPA seemed to enhance the infiltration of ES-ML into cancer tissues.

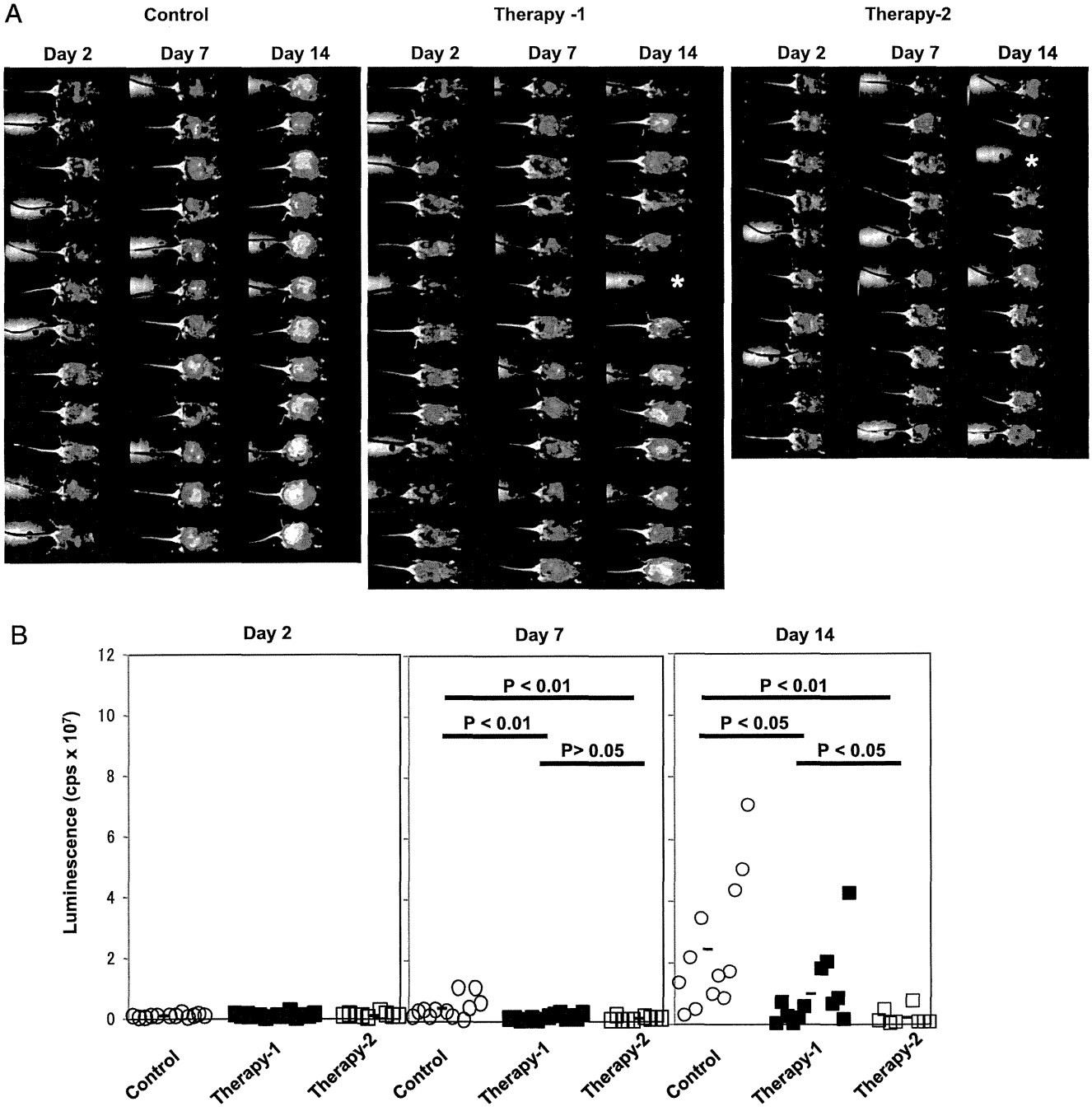

FIGURE 5. Therapeutic effect of coinjection of ES-ML along with IFN-γ plus LPS on peritoneally disseminated cancer. Colon/HL were injected i.p. into CBF1 mice (1×10^6 cells/mouse). On day 2, the mice were subjected to luminescence imaging analysis (**A**) and divided into control [○ in (**B**); $n = 12$], therapy-1 (■; $n = 13$), and therapy-2 (□; $n = 10$) groups. Mice in therapy-1 and -2 groups were injected i.p. with IFN-γ (2×10^4 U) and LPS (1 μg) on days 3, 5, 8, 10, and 12. In addition, mice in therapy-2 group were injected i.p. with ES-ML/anti-HER2 cells (5×10^7), collagenase (20 μg), hyaluronidase (600 μg), and M-CSF (1 μg) on days 2, 4, 7, 9, and 11. To follow the tumor growth, all mice were subjected to bioluminescence analysis on days 7 and 14. (B) Total luminescence signals of individual mice were plotted. One mouse in the therapy-1 group and one mouse in the therapy-2 group died between days 7 and 14 [indicated by asterisks in (A)]. The statistical differences in the values between mouse groups on days 7 and 14 were analyzed using the Mann–Whitney *U* test.

Therapeutic effect of ES-ML with IFN-γ plus LPS on peritoneally disseminated cancer

Based on the cytotoxic effect on Colon/HL by ES-ML stimulated with IFN-γ plus LPS in vitro and the infiltration of exogenously administered ES-ML into cancer tissues in vivo, we expected that administration of ES-ML with IFN-γ plus LPS would exert a therapeutic effect against cancer in vivo.

Colon-26 cells, the parental cells of Colon/HL, were derived from the BALB/c (H-2^d) mouse strain, and the ES-ML used in this study were derived from ES cells of C57BL/6 origin. To avoid immune-mediated rejection of the transferred cancer and ES-ML, we used CBF1 mice as recipients. We injected Colon/HL i.p. into CBF1 mice. After 2 d, we examined the establishment of cancer in the mouse peritoneal cavity by bioluminescence analysis. Mice with established Colon/HL cancer were divided into a control group and two therapy groups. The mice in therapy-1 and -2 groups were injected i.p. with LPS plus IFN-γ three times/week. In addition, mice in therapy-2 group were injected with ES-ML/anti-HER2 cells plus collagenase, hyaluronidase, and M-CSF. Mice in the control group were left untreated. The growth of tumors was monitored by bioluminescence analysis on days 7 and 14. The results of imaging analysis are shown in Fig. 5A, and luminescence counts of individual mice are represented by the dot plots in Fig. 5B.

Cancer growth in the mice in therapy-1 group was significantly inhibited compared with the control group ($p < 0.05$). The cancer-inhibitory effect observed in mice in therapy-1 group may have been exerted by endogenous macrophages stimulated by the administered LPS and IFN-γ. One mouse in the therapy-1 group died between days 7 and 14, probably because of the toxic effect of LPS. Cancer growth in the therapy-2 group was retarded more dramatically than in the therapy-1 group ($p < 0.05$) and the control group ($p < 0.01$), indicating that exogenously transferred ES-ML exerted an anticancer effect. However, one mouse in therapy-2 group also died between days 7 and 14.

Anticancer effect of ES-ML expressing TNF with rIFN-γ

As described above, some of the mice administered LPS plus IFN-γ, with or without ES-ML, died before day 14, probably due to the toxicity of the injected LPS. As shown in Fig. 3B, ES-ML killed Colon/HL in the presence of IFN-γ plus LPS, as well as in the presence of IFN-γ plus TNF. We considered that transfer of ES-ML genetically modified to produce TNF must be less toxic for the mice than injection of LPS or rTNF, because production of TNF by the cancer tissue–infiltrating transfectant ES-ML resulted in more local action of TNF and a lower systemic effect.

We successfully generated transfectant ES-ML producing TNF by lentivirus-mediated transduction (Fig. 6A). Next, we analyzed

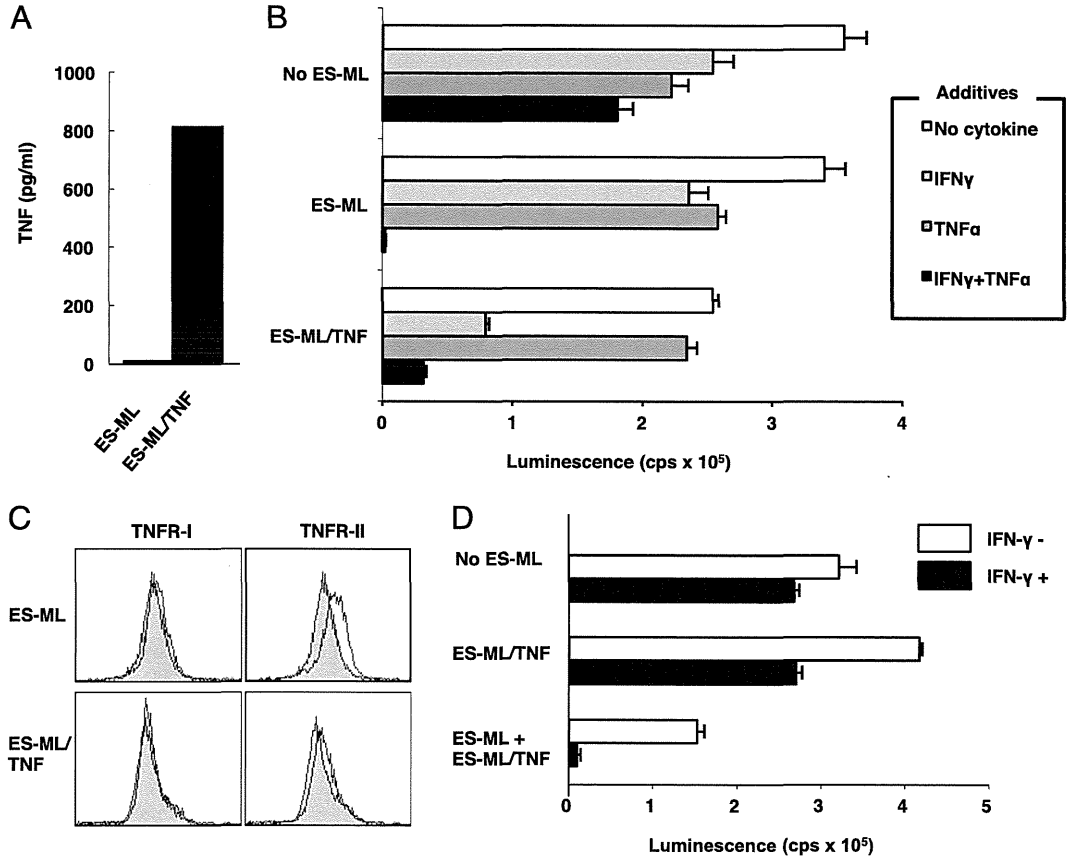

FIGURE 6. Cytotoxicity of ES-ML, with and without production of TNF, against Colon/HL in the presence of IFN-γ. (**A**) ES-ML, with or without TNF transgene, were cultured in a 96-well culture plate (1×10^4 cells/100 μl/well). After 24 h, the culture supernatants were collected, and the concentration of TNF was measured by ELISA. (**B**) Colon/HL (2.5×10^3 cells/well) were cultured alone or cocultured with untransfected ES-ML (1×10^4 cells/well) or ES-ML/TNF (1×10^4 cells/well) in a 96-well culture plate in the absence of cytokine or the presence of IFN-γ (200 U/ml), TNF (10 ng/ml), or IFN-γ plus TNF. The number of live Colon/HL was measured by luciferase activity after 3 d of culture. Data are the mean + SD of triplicate assays. (**C**) Flow cytometric analysis of TNFR-I and -II expression in ES-ML and ES-ML/TNF. The staining profiles of the specific mAb (open graphs) and isotype-matched control mAb (shaded graphs) are shown. (**D**) Colon/HL (2.5×10^3/well) were cultured alone or cocultured with ES-ML/TNF (1×10^4 cells/well) or a combination of ES-ML/TNF (5×10^3 cells/well) and ES-ML (5×10^3 cells/well) in the absence or presence of IFN-γ (200 U/well). The number of live Colon/HL was measured by luciferase activity after 3 d of culture. Data are the mean ± SD of triplicate assays.

the in vitro effect of TNF-transfectant ES-ML (ES-ML/TNF) on Colon/HL in the presence of rIFN-γ. Contrary to our expectation, ES-ML/TNF with rIFN-γ were not as effective as ES-ML with rIFN-γ plus rTNF (Fig. 6B). ES-ML/TNF also were less effective than ES-ML in the presence of rIFN-γ plus rTNF (black bars in Fig. 6B), suggesting that the reactivity of ES-ML/TNF to TNF was lower than that of nontransfected ES-ML. Indeed, expression of TNFR-I and -II in ES-ML/TNF was decreased compared with that in nontransfected ES-ML (Fig. 6C). Probably, cells with lower TNF sensitivity selectively survived during the establishment of ES-ML/TNF. Consistent with these results, in the presence of IFN-γ, the combination of ES-ML/TNF with untransfected ES-ML exhibited more potent cytotoxicity against Colon/HL than did ES-ML/TNF only (Fig. 6D).

Anticancer effect of TAP1-deficient ES-ML in allogeneic mice

We next examined the anticancer effect of ES-ML/TNF in vivo. Because the reactivity of ES-ML/TNF to TNF was impaired, as described above, we simultaneously injected ES-ML/TNF and untransfected ES-ML with rIFN-γ. In these experiments, we used BALB/c mice with an H-2^d MHC haplotype as recipient mice. For the treatments, we used ES-ML derived from TAP1-deficient E14 ES cells (31). Although E14 ES cells originated from the 129/sv strain with an H-2^b MHC haplotype, cell surface expression

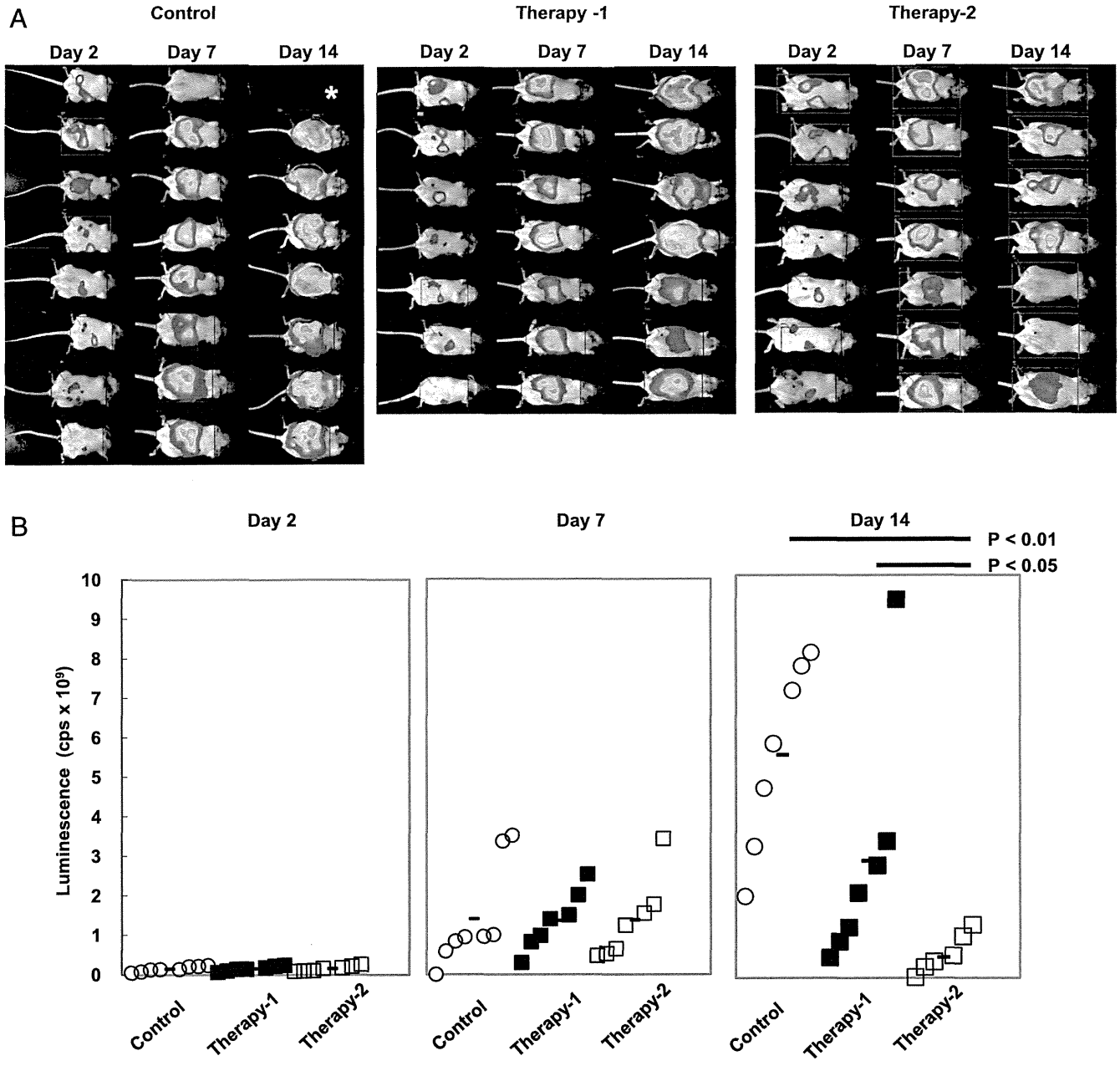

FIGURE 7. Therapeutic effect of TAP1-deficient ES-ML in cancer-bearing allogeneic mice. Colon/HL were injected i.p. into BALB/c mice (2×10^6 cells/mouse). On day 2, the mice were subjected to luminescence imaging analysis (**A**) and divided into control [○ in (**B**), $n = 8$], therapy-1 (■, $n = 7$), and therapy-2 (□, $n = 7$) groups. Mice in therapy-1 group were injected i.p. with IFN-γ (1×10^4 U) twice a week from day 3. Mice in therapy-2 group were injected i.p. with IFN-γ (1×10^4 U) along with TAP1$^{-/-}$ ES-ML ($1–3 \times 10^7$) and TAP1$^{-/-}$ ES-ML/TNF ($1–3 \times 10^7$) twice a week from day 3. To follow the tumor growth, all mice were subjected to bioluminescence analysis on days 7 and 14. (B) Total luminescence signals of individual mice were plotted. One mouse in the control group died between days 7 and 14 [indicated by an asterisk in (A)]. The statistical differences in the value between mouse groups on day 14 were analyzed by the Mann–Whitney *U* test.

of MHC class I was almost completely diminished in TAP1-deficient ES-ML (Supplemental Fig. 2). We expected that, upon injection into BALB/c mice, TAP1-deficient ES-ML could avoid attack by allogeneic MHC class I–reactive CTL, the major effectors in the acute rejection of allogeneic cells, and exert an anticancer effect.

We injected Colon/HL (H-2^d) into BALB/c mice (H-2^d). After 2 d, we examined the establishment of cancer in the mouse peritoneal cavity by bioluminescence analysis. Mice with established Colon/HL cancer were divided into an untreated (control) group and two treatment (therapy-1 and therapy-2) groups. The mice in therapy-1 group were treated with IFN-γ only. Mice in therapy-2 group were treated with ES-ML plus ES-ML/TNF, both TAP1-deficient, along with rIFN-γ. As shown in Fig. 7A and Fig. 7B, cancer progression was significantly inhibited in mice of therapy-2 group compared with those in therapy-1 group ($p < 0.05$) and the control group ($p < 0.01$). Moreover, survival of therapy-2 group mice was significantly extended compared with therapy-1 group and control group mice ($p < 0.01$, Fig. 8).

To investigate malignancy development from TAP-deficient ES-ML in the allogeneic recipients, we injected TAP-deficient ES-ML into BALB/c mice without tumor cell inoculation and observed them for up to 12 wk. During the observation period, mice were completely healthy, and no significant difference in body weight was observed between ES-ML–injected mice and control mice without ES-ML injection (Supplemental Fig. 3). Eight or twelve weeks after the ES-ML injection, the mice were sacrificed, dissected, and examined carefully under a stereomicroscope. We found no difference between ES-ML–inoculated mice and control mice, concluding that no malignancy developed from ES-ML.

These results indicate that, when administered into allogeneic cancer-bearing mice, TAP-deficient ES-ML can overcome the barrier of histoincompatibility and produce a therapeutic effect. Despite the proliferative capacity of ES-ML, TAP-deficient ES-ML did not cause malignancy in the allogeneic recipient mice, indicating that ES-ML therapy is safe in terms of cancer risk.

Discussion

In the current study, we developed a method to generate a large quantity of myeloid cells from mouse ES cells. The myeloid cells with a proliferative capacity, termed ES-ML, exhibited macrophage-like morphology and cell surface markers. ES-ML/anti-HER2 caused a reduction in the number of HER2-expressing Colon-26 cancer cells in coculture experiments. This anticancer effect of ES-ML/anti-HER2 was enhanced by addition of IFN-γ. A more dramatic anti-Colon-26 effect of ES-ML was observed when it was added with IFN-γ plus LPS or IFN-γ plus TNF, resulting in almost complete disappearance of cocultured Colon-26. Although it was suggested that this anticancer effect was mediated, in part, by NO produced by ES-ML, other mechanisms are likely involved. For example, production of molecules with cytotoxic effects, such as reactive oxygen species, proteases, Fas-ligand, TRAIL, and type I IFNs, is a possible mechanism. In addition, phagocytic killing may be involved in the tumor-suppressive effect of macrophages, as we (28) and other investigators (43) previously observed. Exogenously inoculated ES-ML efficiently infiltrated the cancer tissues in mice. Administration of ES-ML with IFN-γ plus LPS inhibited the growth of pre-established Colon/HL cancer in the peritoneal cavity of the mice.

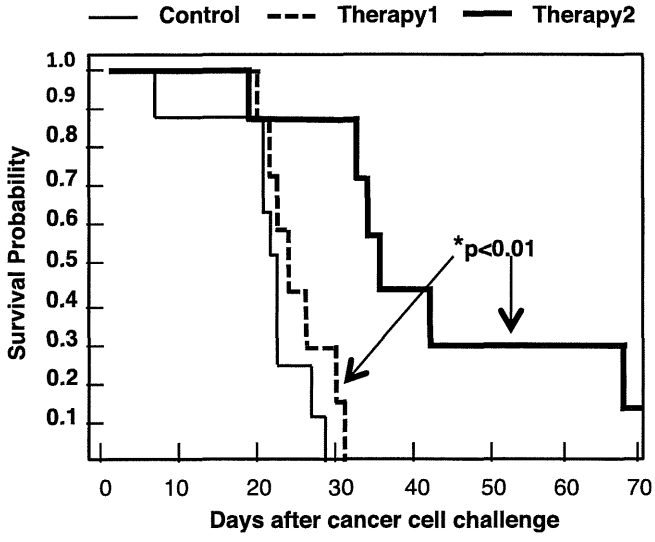

FIGURE 8. Survival of cancer-inoculated mice. Survival curves of control, therapy-1, and therapy-2 mouse groups. The differences between therapy-2 and control groups, as well as between therapy-2 and therapy-1 groups, were statistically significant (log-rank test, both $p < 0.01$).

We also recently developed a method to generate myeloid cells with a proliferative capacity from human iPS cells (44, 45). iPS cell–derived proliferating myeloid cell lines (iPS-ML) were generated by introducing proliferation and antisenescence factors (e.g., cMYC and BMI1) into human iPS cell–derived myeloid cells, and they grew continuously in an M-CSF–dependent manner. This technique enabled us to generate a large quantity of human cells exhibiting macrophage-like properties. We observed that iPS-ML genetically modified to express IFN-β significantly inhibited the growth of human gastric and pancreatic cancers in xenograft models using SCID mice (45). However, there are several drawbacks related to the application of iPS-ML in practical medicine. The generation of patient-specific iPS-ML may be very expensive, and >2 mo are necessary to establish iPS cells and subsequently generate iPS-ML. A more critical issue is the risk for developing malignancy after administration of autologous iPS-ML to patients.

TAP is a dimer composed of TAP1 and TAP2 molecules, and it plays a key role in the supply of antigenic peptides to the HLA class I pathway (46). In TAP-deficient cells, cell surface expression of HLA class I, as well as the diversity of peptides presented by HLA class I molecules, is very low. Thus, we expect that TAP-deficient allogeneic iPS-ML evade recognition by most allo-MHC class I–reactive CTL that play a major role in the acute rejection of transferred allogeneic cells (47, 48). Nevertheless, the alloreactive CTL recognizing HLA class I–bound peptides presented via the TAP-independent pathway, which are mainly derived from signal peptides of membrane or secreted proteins (49), may eventually eliminate the transferred allogeneic iPS-ML cells. Collectively, TAP-deficient allogeneic iPS-ML may survive in recipients for a certain duration and exert their anticancer effects, but eventually they would be eliminated by the immune system. Therefore, we presume that therapies using allogeneic TAP-deficient iPS-ML cells may be effective and safe.

In the current study, we evaluated this concept using a mouse model. We generated ES-ML from TAP1-deficient mouse E14 ES cells derived from the 129/sv strain with an H-2^b MHC haplotype. We demonstrated that treatment of cancer-bearing BALB/c mice (H-2^d) with TAP1-deficient ES-ML, with and without production of TNF, plus IFN-γ resulted in significant inhibition of cancer progression (Fig. 7), as well as prolongation of mouse survival (Fig. 8). These results indicate that TAP-deficient ES-ML can act as anticancer effector cells in H-2–mismatched recipients. Furthermore, as indicated by Supplemental Fig. 3, even if $>1.5 \times 10^8$ ES-ML were administered per mouse in total, we never observed development of malignancies from the transferred ES-ML.

The present study demonstrated that anticancer therapy using allogeneic TAP-deficient pluripotent stem cell–derived proliferating macrophages is effective and safe. We observed no malignancy development from TAP-mutated ES-ML after transfer to allogeneic recipient mice, as shown in Supplemental Fig. 3. We are planning a similar preclinical study using nonhuman primates to further evaluate the safety of macrophage therapy. Cancer therapy strategies using other cell types with tumor tropism, such as mesenchymal stem cells and neural stem cells, have been reported (50–53). These strategies will be evaluated further for their efficacy and safety in preclinical and clinical studies in the near future.

Disclosures

The authors have no financial conflicts of interest.

References

1. Lewis, C. E., and J. W. Pollard. 2006. Distinct role of macrophages in different tumor microenvironments. *Cancer Res.* 66: 605–612.
2. De Palma, M., and C. E. Lewis. 2013. Macrophage regulation of tumor responses to anticancer therapies. *Cancer Cell* 23: 277–286.
3. Coussens, L. M., L. Zitvogel, and A. K. Palucka. 2013. Neutralizing tumor-promoting chronic inflammation: a magic bullet? *Science* 339: 286–291.
4. Mantovani, A., T. Schioppa, C. Porta, P. Allavena, and A. Sica. 2006. Role of tumor-associated macrophages in tumor progression and invasion. *Cancer Metastasis Rev.* 25: 315–322.
5. Sica, A., and V. Bronte. 2007. Altered macrophage differentiation and immune dysfunction in tumor development. *J. Clin. Invest.* 117: 1155–1166.
6. Sica, A., and A. Mantovani. 2012. Macrophage plasticity and polarization: in vivo veritas. *J. Clin. Invest.* 122: 787–795.
7. Tsujikawa, T., T. Yaguchi, G. Ohmura, S. Ohta, A. Kobayashi, N. Kawamura, T. Fujita, H. Nakano, T. Shimada, T. Takahashi, et al. 2013. Autocrine and paracrine loops between cancer cells and macrophages promote lymph node metastasis via CCR4/CCL22 in head and neck squamous cell carcinoma. *Int. J. Cancer* 132: 2755–2766.
8. Bonnotte, B., N. Larmonier, N. Favre, A. Fromentin, M. Moutet, M. Martin, S. Gurbuxani, E. Solary, B. Chauffert, and F. Martin. 2001. Identification of tumor-infiltrating macrophages as the killers of tumor cells after immunization in a rat model system. *J. Immunol.* 167: 5077–5083.
9. Guiducci, C., A. P. Vicari, S. Sangaletti, G. Trinchieri, and M. P. Colombo. 2005. Redirecting in vivo elicited tumor infiltrating macrophages and dendritic cells towards tumor rejection. *Cancer Res.* 65: 3437–3446.
10. Hagemann, T., T. Lawrence, I. McNeish, K. A. Charles, H. Kulbe, R. G. Thompson, S. C. Robinson, and F. R. Balkwill. 2008. "Re-educating" tumor-associated macrophages by targeting NF-kappaB. *J. Exp. Med.* 205: 1261–1268.
11. Dace, D. S., P. W. Chen, and J. Y. Niederkorn. 2008. CD4+ T-cell-dependent tumour rejection in an immune-privileged environment requires macrophages. *Immunology* 123: 367–377.
12. Menon, C., T. W. Bauer, S. T. Kelley, D. J. Raz, J. I. Bleier, K. Patel, K. Steele, I. Prabakaran, A. Shifrin, D. G. Buerk, et al. 2008. Tumoricidal activity of high-dose tumor necrosis factor-alpha is mediated by macrophage-derived nitric oxide burst and permanent blood flow shutdown. *Int. J. Cancer* 123: 464–475.
13. Ho, T. C., S. L. Chen, S. C. Shih, S. J. Chang, S. L. Yang, J. W. Hsieh, H. C. Cheng, L. J. Chen, and Y. P. Tsao. 2011. Pigment epithelium-derived factor (PEDF) promotes tumor cell death by inducing macrophage membrane tumor necrosis factor-related apoptosis-inducing ligand (TRAIL). *J. Biol. Chem.* 286: 35943–35954.
14. Beatty, G. L., E. G. Chiorean, M. P. Fishman, B. Saboury, U. R. Teitelbaum, W. Sun, R. D. Huhn, W. Song, D. Li, L. L. Sharp, et al. 2011. CD40 agonists alter tumor stroma and show efficacy against pancreatic carcinoma in mice and humans. *Science* 331: 1612–1616.
15. Shirota, Y., H. Shirota, and D. M. Klinman. 2012. Intratumoral injection of CpG oligonucleotides induces the differentiation and reduces the immunosuppressive activity of myeloid-derived suppressor cells. *J. Immunol.* 188: 1592–1599.
16. Shime, H., M. Matsumoto, H. Oshiumi, S. Tanaka, A. Nakane, Y. Iwakura, H. Tahara, N. Inoue, and T. Seya. 2012. Toll-like receptor 3 signaling converts tumor-supporting myeloid cells to tumoricidal effectors. *Proc. Natl. Acad. Sci. USA* 109: 2066–2071.
17. Movahedi, K., D. Laoui, C. Gysemans, M. Baeten, G. Stangé, J. Van den Bossche, M. Mack, D. Pipeleers, P. In't Veld, P. De Baetselier, and J. A. Van Ginderachter. 2010. Different tumor microenvironments contain functionally distinct subsets of macrophages derived from Ly6C(high) monocytes. *Cancer Res.* 70: 5728–5739.
18. Murray, P. J., and T. A. Wynn. 2011. Protective and pathogenic functions of macrophage subsets. *Nat. Rev. Immunol.* 11: 723–737.
19. Faradji, A., A. Bohbot, M. Schmitt-Goguel, N. Roeslin, S. Dumont, M. L. Wiesel, C. Lallot, M. Eber, J. Bartholeyns, P. Poindron, et al. 1991. Phase I trial of intravenous infusion of ex-vivo-activated autologous blood-derived macrophages in patients with non-small-cell lung cancer: toxicity and immunomodulatory effects. *Cancer Immunol. Immunother.* 33: 319–326.
20. Lopez, M., J. Fechtenbaum, B. David, C. Martinache, M. Chokri, S. Canepa, A. De Gramont, C. Louvet, I. Gorin, O. Mortel, and J. Bartholeyns. 1992. Adoptive immunotherapy with activated macrophages grown in vitro from blood monocytes in cancer patients: a pilot study. *J. Immunother.* 11: 209–217.
21. Andreesen, R., C. Scheibenbogen, W. Brugger, S. Krause, H. G. Meerpohl, H. G. Leser, H. Engler, and G. W. Löhr. 1990. Adoptive transfer of tumor cytotoxic macrophages generated in vitro from circulating blood monocytes: a new approach to cancer immunotherapy. *Cancer Res.* 50: 7450–7456.
22. Baron-Bodo, V., P. Doceur, M. L. Lefebvre, K. Labroquère, C. Defaye, C. Cambouris, D. Prigent, M. Salcedo, A. Boyer, and A. Nardin. 2005. Antitumor properties of human-activated macrophages produced in large scale for clinical application. *Immunobiology* 210: 267–277.
23. Klimp, A. H., E. G. de Vries, G. L. Scherphof, and T. Daemen. 2002. A potential role of macrophage activation in the treatment of cancer. *Crit. Rev. Oncol. Hematol.* 44: 143–161.
24. Monnet, I., J. L. Breau, D. Moro, H. Lena, J. C. Eymard, O. Ménard, J. P. Vuillez, M. Chokri, J. L. Romet-Lemonne, and M. Lopez. 2002. Intrapleural infusion of activated macrophages and gamma-interferon in malignant pleural mesothelioma: a phase II study. *Chest* 121: 1921–1927.
25. Hennemann, B., A. Rehm, A. Kottke, N. Meidenbauer, and R. Andreesen. 1997. Adoptive immunotherapy with tumor-cytotoxic macrophages derived from recombinant human granulocyte-macrophage colony-stimulating factor (rhuGM-CSF) mobilized peripheral blood monocytes. *J. Immunother.* 20: 365–371.
26. Takahashi, K., K. Tanabe, M. Ohnuki, M. Narita, T. Ichisaka, K. Tomoda, and S. Yamanaka. 2007. Induction of pluripotent stem cells from adult human fibroblasts by defined factors. *Cell* 131: 861–872.
27. Senju, S., M. Haruta, Y. Matsunaga, S. Fukushima, T. Ikeda, K. Takahashi, K. Okita, S. Yamanaka, and Y. Nishimura. 2009. Characterization of dendritic cells and macrophages generated by directed differentiation from mouse induced pluripotent stem cells. *Stem Cells* 27: 1021–1031.
28. Senju, S., M. Haruta, K. Matsumura, Y. Matsunaga, S. Fukushima, T. Ikeda, K. Takamatsu, A. Irie, and Y. Nishimura. 2011. Generation of dendritic cells and macrophages from human induced pluripotent stem cells aiming at cell therapy. *Gene Ther.* 18: 874–883.
29. Choi, K. D., M. A. Vodyanik, and I. I. Slukvin. 2009. Generation of mature human myelomonocytic cells through expansion and differentiation of pluripotent stem cell-derived lin-CD34+CD43+CD45+ progenitors. *J. Clin. Invest.* 119: 2818–2829.
30. Yanagimachi, M. D., A. Niwa, T. Tanaka, F. Honda-Ozaki, S. Nishimoto, Y. Murata, T. Yasumi, J. Ito, S. Tomida, K. Oshima, et al. 2013. Robust and highly-efficient differentiation of functional monocytic cells from human pluripotent stem cells under serum- and feeder cell-free conditions. *PLoS ONE* 8: e59243.
31. Matsunaga, Y., D. Fukuma, S. Hirata, S. Fukushima, M. Haruta, T. Ikeda, I. Negishi, Y. Nishimura, and S. Senju. 2008. Activation of antigen-specific cytotoxic T lymphocytes by beta 2-microglobulin or TAP1 gene disruption and the introduction of recipient-matched MHC class I gene in allogeneic embryonic stem cell-derived dendritic cells. *J. Immunol.* 181: 6635–6643.
32. Senju, S., S. Hirata, H. Matsuyoshi, M. Masuda, Y. Uemura, K. Araki, K. Yamamura, and Y. Nishimura. 2003. Generation and genetic modification of dendritic cells derived from mouse embryonic stem cells. *Blood* 101: 3501–3508.
33. Song, E., P. Zhu, S. K. Lee, D. Chowdhury, S. Kussman, D. M. Dykxhoorn, Y. Feng, D. Palliser, D. B. Weiner, P. Shankar, et al. 2005. Antibody mediated in vivo delivery of small interfering RNAs via cell-surface receptors. *Nat. Biotechnol.* 23: 709–717.
34. Miyoshi, H., U. Blömer, M. Takahashi, F. H. Gage, and I. M. Verma. 1998. Development of a self-inactivating lentivirus vector. *J. Virol.* 72: 8150–8157.
35. Cohen, J. A., D. B. Weiner, K. F. More, Y. Kokai, W. V. Williams, H. C. Maguire, Jr., V. A. LiVolsi, and M. I. Greene. 1989. Expression pattern of the neu (NGL) gene-encoded growth factor receptor protein (p185neu) in normal and transformed epithelial tissues of the digestive tract. *Oncogene* 4: 81–88.
36. Kuwada, S. K., C. L. Scaife, J. Kuang, X. Li, R. F. Wong, S. R. Florell, R. J. Coffey, Jr., and P. D. Gray. 2004. Effects of trastuzumab on epidermal growth factor receptor-dependent and -independent human colon cancer cells. *Int. J. Cancer* 109: 291–301.
37. Carter, P., L. Presta, C. M. Gorman, J. B. Ridgway, D. Henner, W. L. Wong, A. M. Rowland, C. Kotts, M. E. Carver, and H. M. Shepard. 1992. Humanization of an anti-p185HER2 antibody for human cancer therapy. *Proc. Natl. Acad. Sci. USA* 89: 4285–4289.
38. Gravalos, C., and A. Jimeno. 2008. HER2 in gastric cancer: a new prognostic factor and a novel therapeutic target. *Ann. Oncol.* 19: 1523–1529.
39. Iannello, A., and A. Ahmad. 2005. Role of antibody-dependent cell-mediated cytotoxicity in the efficacy of therapeutic anti-cancer monoclonal antibodies. *Cancer Metastasis Rev.* 24: 487–499.
40. Stuehr, D. J., and M. A. Marletta. 1987. Induction of nitrite/nitrate synthesis in murine macrophages by BCG infection, lymphokines, or interferon-gamma. *J. Immunol.* 139: 518–525.
41. Ding, A. H., C. F. Nathan, and D. J. Stuehr. 1988. Release of reactive nitrogen intermediates and reactive oxygen intermediates from mouse peritoneal macrophages. Comparison of activating cytokines and evidence for independent production. *J. Immunol.* 141: 2407–2412.
42. Rees, D. D., R. M. Palmer, H. F. Hodson, and S. Moncada. 1989. A specific inhibitor of nitric oxide formation from L-arginine attenuates endothelium-dependent relaxation. *Br. J. Pharmacol.* 96: 418–424.

43. Pallasch, C. P., I. Leskov, C. J. Braun, D. Vorholt, A. Drake, Y. M. Soto-Feliciano, E. H. Bent, J. Schwamb, B. Iliopoulou, N. Kutsch, et al. 2014. Sensitizing protective tumor microenvironments to antibody-mediated therapy. *Cell* 156: 590–602.
44. Haruta, M., Y. Tomita, A. Yuno, K. Matsumura, T. Ikeda, K. Takamatsu, E. Haga, C. Koba, Y. Nishimura, and S. Senju. 2013. TAP-deficient human iPS cell-derived myeloid cell lines as unlimited cell source for dendritic cell-like antigen-presenting cells. *Gene Ther.* 20: 504–513.
45. Koba, C., M. Haruta, Y. Matsunaga, K. Matsumura, E. Haga, Y. Sasaki, T. Ikeda, K. Takamatsu, Y. Nishimura, and S. Senju. 2013. Therapeutic effect of human iPS-cell-derived myeloid cells expressing IFN-β against peritoneally disseminated cancer in xenograft models. *PLoS ONE* 8: e67567.
46. Neefjes, J. J., F. Momburg, and G. J. Hämmerling. 1993. Selective and ATP-dependent translocation of peptides by the MHC-encoded transporter. *Science* 261: 769–771.
47. Loyer, V., P. Fontaine, S. Pion, F. Hétu, D. C. Roy, and C. Perreault. 1999. The in vivo fate of APCs displaying minor H antigen and/or MHC differences is regulated by CTLs specific for immunodominant class I-associated epitopes. *J. Immunol.* 163: 6462–6467.
48. Hermans, I. F., D. S. Ritchie, J. Yang, J. M. Roberts, and F. Ronchese. 2000. CD8 + T cell-dependent elimination of dendritic cells in vivo limits the induction of antitumor immunity. *J. Immunol.* 164: 3095–3101.
49. Bacik, I., J. H. Cox, R. Anderson, J. W. Yewdell, and J. R. Bennink. 1994. TAP (transporter associated with antigen processing)-independent presentation of endogenously synthesized peptides is enhanced by endoplasmic reticulum insertion sequences located at the amino- but not carboxyl-terminus of the peptide. *J. Immunol.* 152: 381–387.
50. Studeny, M., F. C. Marini, R. E. Champlin, C. Zompetta, I. J. Fidler, and M. Andreeff. 2002. Bone marrow-derived mesenchymal stem cells as vehicles for interferon-beta delivery into tumors. *Cancer Res.* 62: 3603–3608.
51. Hall, B., J. Dembinski, A. K. Sasser, M. Studeny, M. Andreeff, and F. Marini. 2007. Mesenchymal stem cells in cancer: tumor-associated fibroblasts and cell-based delivery vehicles. *Int. J. Hematol.* 86: 8–16.
52. Aboody, K. S., J. Najbauer, and M. K. Danks. 2008. Stem and progenitor cell-mediated tumor selective gene therapy. *Gene Ther.* 15: 739–752.
53. Ren, C., S. Kumar, D. Chanda, J. Chen, J. D. Mountz, and S. Ponnazhagan. 2008. Therapeutic potential of mesenchymal stem cells producing interferon-alpha in a mouse melanoma lung metastasis model. *Stem Cells* 26: 2332–2338.

Identification of a novel HLA-A*02:01-restricted cytotoxic T lymphocyte epitope derived from the EML4-ALK fusion gene

MAYUKO YOSHIMURA[1,2], YOSHITAKA TADA[1,3], KAZUYA OFUZI[1], MASAKAZU YAMAMOTO[2] and TETSUYA NAKATSURA[1,3]

[1]Division of Cancer Immunotherapy, Exploratory Oncology Research and Clinical Trial Center, National Cancer Center, Kashiwa, Chiba 277-8577; [2]Department of Gastroenterological Surgery, Tokyo Women's Medical University, Shinzyukuku, Tokyo 162-8666; [3]Research Institute for Biomedical Sciences, Tokyo University of Science, Chiba 278-0022, Japan

Received March 21, 2014; Accepted April 23, 2014

DOI: 10.3892/or.2014.3198

Abstract. Cancer immunotherapy is a promising new approach to cancer treatment. It has been demonstrated that a high number of tumor-specific cytotoxic T cells (CTLs) is associated with increased disease-specific survival in lung cancer patients. Identification of superior CTL epitopes from tumor antigens is essential for the development of immunotherapy for malignant tumors. The EML4-ALK fusion gene was recently identified in a subset of non-small cell lung cancers (NSCLCs). In this study we searched for HLA-A*02:01- and HLA-A*24:02-restricted epitopes derived from EML4-ALK by screening predicted EML4-ALK-derived candidate peptides for the induction of tumor-reactive CTLs. Nine EML4-ALK-derived peptides were selected by a computer algorithm based on a permissive HLA-A*02:01 or HLA-A*24:02 binding motif. One of the nine peptides induced peptide-specific CTLs from human peripheral blood mononuclear cells. We were able to generate a peptide-specific CTL clone. This CTL clone specifically recognized peptide-pulsed T2 cells and H2228 cells expressing HLA-A*02:01 and EML4-ALK that had been treated with IFN-γ 48 h prior to examination. CTL activity was inhibited by an anti-HLA-class I monoclonal antibody (W6/32), consistent with a class I-restricted mechanism of cytotoxicity. These results suggest that this peptide (RLSALESRV) is a novel HLA-A*02:01-restricted CTL epitope and that it may be a new target for antigen-specific immunotherapy against EML4-ALK-positive cancers.

Introduction

Lung cancer is one of the main causes of cancer-related mortality. Approximately 85% of lung cancers are diagnosed as non-small cell lung cancer (NSCLC), and the overall survival (OS) rate for advanced NSCLC is poor. The 5-year survival rate is 5% for stage IIIb NSCLC and <1% for stage IV NSCLC (1). Treatment for NCSLC is determined by the patient's clinical and tumor characteristics, performance status (PS), the histological subtype and tumor genotype/phenotype.

Recently, there have been many studies concerning agents that target molecular changes, such as mutations in the epidermal growth factor receptor (EGFR) and the fusion oncogene EML4-ALK, in which the echinoderm microtubule-associated protein-like 4 (EML4) is fused with the intracellular domain of anaplastic kinase (ALK) (2-4). Although significant advances have been made in the treatment of NSCLC using molecular targeted therapies such as erlotinib and crizotinib, the median OS for patients with advanced NSCLC remains low (5,6), and acquired resistance to target agents is a major clinical problem. Therefore, the development of novel therapies is needed (7).

Immunotherapy manipulates the immune system to control and eradicate cancer. Many recent studies provide evidence suggesting that immunotherapeutic manipulations are viable in many tumor types, including lung cancer. Numerous trials of peptide vaccines, autologous cellular therapy, T cell-directed antibody therapy and monoclonal antibody therapy for lung cancer have been carried out around the world (8-10) and some of them have shown favorable results (11-13).

The EML4-ALK fusion gene was identified in NSCLC patients by a team led by Professor H. Mano. This fusion gene was formed as the result of a small inversion within the short arm of chromosome 2 that joins differing portions of the EML4 gene with a portion of the ALK gene (14,15). As a result of this fusion, constant dimerization of the kinase domain of ALK is induced and its catalytic activity increases consequently.

The EML4-ALK fusion gene is mainly identified in young, never/former light smokers with NSCLC (16). It is estimated that approximately 5% of all NSCLC cases have this fusion gene. A few reports have also identified EML4-ALK in other cancers, namely breast cancer and colorectal cancer (17,18). For the most part, the EML4-ALK fusion gene and other mutations, such as those in EGFR and KRAS, are mutually exclusive (19).

Correspondence to: Dr Tetsuya Nakatsura, Division of Cancer Immunotherapy, Exploratory Oncology Research and Clinical Trial Center, National Cancer Center, 6-5-1 Kashiwanoha, Kashiwa, Chiba 277-8577, Japan
E-mail: tnakatsu@east.ncc.go.jp

Key words: EML4-ALK, peptide vaccine, CTL clone, lung cancer

The chromosomal inversion does not always occur in the same location, and multiple EML4-ALK variants have been identified (19). At least 11 variants have been reported. The most common variants are E13;A20 (variant 1) and E6a/b;A20 (variant 3a/b), which have been detected in 33% and 29% of NSCLC patients, respectively (14).

PF-02341066 (crizotinib) is an ALK inhibitor currently under clinical development. Kwak *et al* conducted an open-label, multi-center, two-part phase I trial and found a remarkable 57% overall response rate and a 72% 6-month progression-free survival rate (20).

In spite of the marked antitumor activity of crizotinib, ALK-positive cancers invariably gain resistance to crizotinib. In the case of ALK-positive cancers, as well as EGFR-mutant lung cancer, resistance develops on average within the first 2 years of therapy (21). The main resistance mutations are L1196M, a gatekeeper mutation and C1156M. In addition to ALK mutations, other known mechanisms for acquired resistance include ALK amplification (21,22) and EGFR activation (23,24). To overcome resistance, new ALK inhibitors are currently in early phase studies (25). Novel combinatorial strategies to overcome crizotinib resistance and further improve the clinical outcome are needed.

We focused on this new fusion array as a novel target of immunotherapy. There are several methods to detect EML4-ALK NSCLC, including polymerase chain reaction (PCR), immunohistochemistry (IHC) and fluorescence in situ hybridization (FISH) (19). These methods detect high-level EML4-ALK fusion gene expression. Passoni *et al* identified two HLA-A*02:01-restricted ALK-derived peptides that induce peptide-specific CTL lines (26).

We focused on the EML4 array as a novel epitope of immunotherapy. We identified a candidate 9- or 10-amino acid array of novel epitopes using the Bioinformatics and Molecular Analysis Section (BIMAS) software and analyzed its potential as a new immunotherapy epitope, with respect to its ability to induce anticancer activity. We then induced and generated a peptide-specific CTL clone from peripheral blood lymphocytes of HLA-A*02:01-positive healthy donors. We report here that an EML4-ALK-derived peptide-specific human CTL clone recognized peptide-pulsed T2 cells and HLA-A*02:01-positive and EML4-ALK-positive tumor cells pretreated with IFN-γ. Furthermore, we showed that immunotherapy with this novel epitope peptide has potential for treatment of EML4-ALK-positive NSCLC.

Materials and methods

Peptides. Human EML4-ALK-derived peptides carrying binding motifs for HLA-A*02:01-/HLA-A*24:02-encoded molecules were identified by HLA-peptide binding predictions using the BIMAS program (http://bimas.dcrt.nih.gov/molbio/hla_bind/index.html). We purchased a total of seven EML4-ALK-derived peptides carrying HLA-A*02:01 binding motifs and two peptides carrying HLA-A*24:02 binding motifs from Geneworld (Tokyo, Japan).

Cell lines. The H2228 human lung adenocarcinoma cell line and EML4-ALK fusion protein variant 3 (E6;A20) were kindly provided by Professor S. Yano (Kanazawa University).

T2 is a lymphoblastoid cell line that lacks TAP function and has HLA-A*02:01 molecules that can easily be loaded with exogenous peptides. T2A24 is the same cell line but with HLA-A*24:02 instead. T2 and T2A24 cells were cultured in RPMI medium supplemented with 10% heat-inactivated FBS.

*HLA-A*02:01/HLA-A*24:02 binding assay*. In order to determine the binding ability of the predicted peptides to HLA-A*02:01/HLA-A*24:02 molecules, an *in vitro* cellular binding assay was performed as reported previously (27).

Briefly, after incubation of the T2/T2A24 cells in culture medium at 26˚C for 18 h, cells were washed with PBS and suspended in 1 ml Opti-MEM (Invitrogen, Carlsbad, CA, USA) with or without 100 μg peptide and then incubated at 26˚C for 3 h and at 37˚C for 3 h. After washing with PBS, HLA-A*02:01/HLA-A*24:02 expression was measured by flow cytometry using a FITC-conjugated and HLA-A*02:01-/HLA-A*24:02-specific monoclonal antibody (mAb) and the mean fluorescence intensity was recorded.

Generation of dendritic cells. $CD14^+$ cells were isolated from human peripheral blood mononuclear cells (PBMCs) using human CD14 microbeads (Miltenyi Biotec, Bergisch Gladbach, Germany). Immature dendritic cells (DCs) were generated from $CD14^+$ cells using interleukin (IL)-4 (10 ng/ml; PeproTech Inc., Rocky Hill, NJ, USA) and granulocyte-macrophage colony-stimulating factor (GM-CSF; 10 ng/ml; PeproTech) in RPMI-1640 medium supplemented with 10% FBS. Maturation of DCs was induced by prostaglandin E2 (PGE2; 1 μg/ml; Sigma, St. Louis, MO, USA) and tumor necrosis factor (TNF-)-α (10 ng/ml; PeproTech).

Induction of EML4-ALK-derived peptide-specific CTLs from PBMCs. $CD8^+$ cells were isolated from PBMCs using human CD8 microbeads (Miltenyi Biotec, Bergisch Gladbach, Germany). $CD8^+$ cells ($2x10^6$) were stimulated by peptide-pulsed irradiated autologous mature DCs ($1x10^5$). Autologous DCs were prepared from a limited supply; artificial antigen presenting cells (aAPCs) (K562/A2 or A24/CD80/CD83) were alternatively used for further examination. After 1 week, these cells were stimulated twice per week by peptide-pulsed irradiated artificial APC-A2 or artificial APC-A24 cells ($1x10^5$). Supplementation with 10 IU/ml IL-2 (Proleukin; Novartis Pharmaceuticals, Basel, Switzerland) and 10 ng/ml IL-15 (PeproTech) was performed every 3 to 4 days between stimulations (28).

IFN-γ ELISPOT assay. Specific secretion of IFN-γ from human CTLs in response to stimulator cells was assayed using the IFN-γ ELISPOT kit (BD Biosciences), according to the manufacturer's instructions. Stimulator cells were pulsed with peptide for 2 h at room temperature and then washed. Responder cells were incubated with stimulator cells for 20 h. The resulting spots were counted using an ELIPHOTO counter (Minerva Tech, Tokyo, Japan). HIV-gag (77-85) (SLYNTYATL) was used as an irrelevant peptide in the CTL assay.

Generation of CTL clones. Cultured cells were incubated with peptide-pulsed T2/T2A24 cells at a ratio of 2:1 for 3.5 h

Table I. HLA-A2 peptide binding predictions of the BIMAS program.

Peptide name	Peptide sequence	Binding score[a]
A	RLSALESRV	69.552
B	AISEDHVASV	90.183
C	TVLKAALADV	51.79
D	KLIPKVTKT	59.989
E	YLLPTGEIV	237.82
F	MLIWSKTTV	118.238
G	VMLIWSKTTV	315.95

[a]Binding scores were estimated using BIMAS software (http://www-bimas.cit.nih.gov/mobio/hla_bind/).

Table II. HLA-A24 peptide binding predictions of the BIMAS program.

Peptide name	Peptide sequence	Binding score[a]
H	NYDDIRTEL	369.6
I	VYFIASVVVL	200

[a]Binding scores were estimated using BIMAS software (http://www-bimas.cit.nih.gov/mobio/hla_bind/).

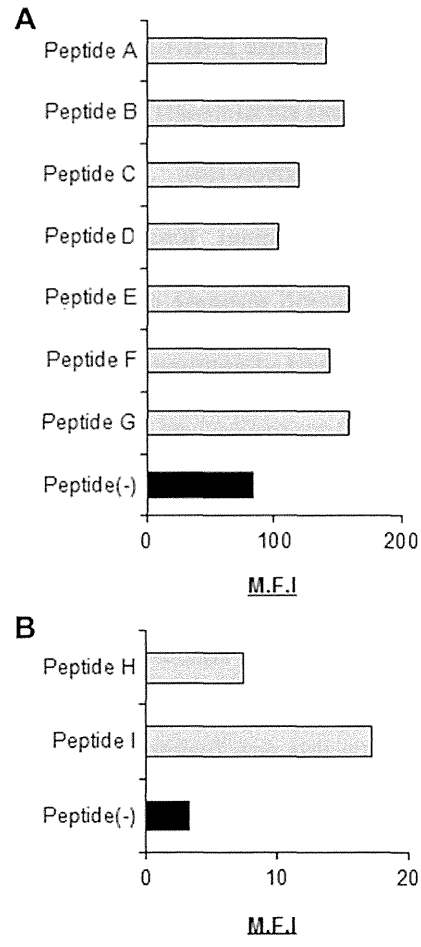

Figure 1. EML4-ALK-derived peptides bound to HLA-A2 or HLA-A24 molecules. *In vitro* cellular peptide binding assays for HLA-A*02:01 (A) or HLA-A*24:02 (B) were performed using a FACS system.

at 37°C. CD107a-specific antibodies (BioLegend, San Diego, CA, USA) were included in the mixture during the incubation period. $CD8^+CD107a^+$ cells were sorted using a FACSAria II cell sorter (BD Biosciences). Sorted CTLs were stimulated and the CTL clones were established as described previously (29).

Flow cytometry. H2228 cells with or without pretreatment with 100 U/ml IFN-γ (PeproTech) for 48 h were harvested and stained with anti-HLA-A2 Ab-FITC (MBL, Japan) and analyzed using a FACSCanto II flow cytometer (BD Biosciences). Flow cytometry data were analyzed using FlowJo software.

Cytotoxicity assay. The cytotoxic capacity was analyzed using the Terascan VPC system (Minerva Tech, Tokyo). The CTL clone was used as the effector cell type. Target cells treated with 100 U/ml IFN-γ (PeproTech) 42 h previously were labeled through incubation in calcein-AM solution for 30 min at 37°C. The labeled cells ($1x10^4$) were then co-cultured with the effector cells for 4-6 h. Fluorescence intensity was measured before and after the culture period, and specific cytotoxic activity was calculated as described previously (29).

HLA-A*02:01 blocking of T-cell activity was tested by pre-incubating the target cells with anti-HLA-A, -B, -C mAb (W6/32) or an isotype control mAb (mIgG2a,κ; BioLegend San Diego, CA, USA).

Results

*Identification of HLA-A*02:01-/HLA-A*24:02-restricted EML4-ALK-derived peptides*. As candidate EML4-ALK-derived and HLA-A*02:01-/HLA-A*24:02-restricted CTL epitopes, we selected nine peptides with highly predicted scores for HLA-A*02:01/HLA-A*24:02 binding calculated using BIMAS software (Tables I and II) and evaluated their ability to bind to HLA-A*02:01/HLA-A*24:02 molecules. All nine peptides were able to bind HLA-A*02:01/HLA-A*24:02 molecules (Fig. 1).

Generation of an EML4-ALK-derived peptide-specific CTL clone from human PBMCs. We next assessed the capacity of EML4-ALK-derived peptides to generate peptide-specific CTLs *in vitro* from human PBMCs of HLA-A*02:01/HLA-A*24:02 healthy donors. CTLs were induced by three stimulations with DCs or artificial APCs loaded with the EML4-ALK-derived peptides. CTLs were tested for specificity for each peptide using the IFN-γ ELISPOT assay. Peptides A, B and C could induce peptide-specific CTLs that were able to specifically recognize T2 cells pulsed with each peptide, but not T2 cells without peptides (Fig. 2). Peptides B and C were able to induce CTLs from only one donor (healthy donor 3 for peptide B and healthy donor 4 for

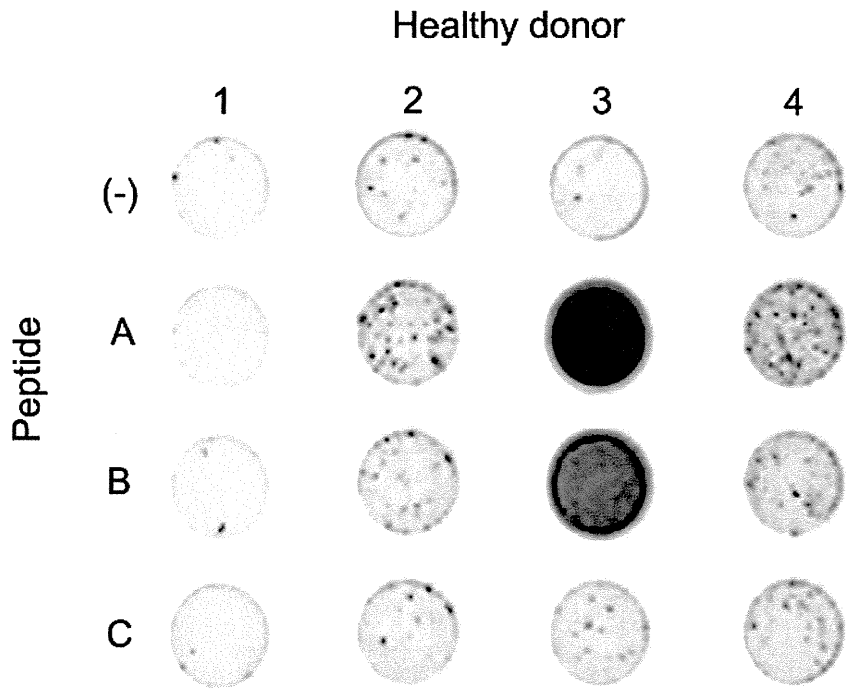

Figure 2. IFN-γ release by *in vitro*-induced anti-EML4-ALK CTLs. $CD8^+$ T cells from four healthy donors were stimulated with EML4-ALK-derived peptide-pulsed autologous DCs and aAPCs. CTLs induced by EML4-ALK-derived peptides ($1x10^5$) were stimulated with T2 cells pulsed with or without 1 μM EML4-ALK-derived peptides. IFN-γ-producing CTLs were detected by IFN-γ ELISPOT assay. DCs, dendritic cells; aAPCs, artificial antigen presenting cells; CTLs, cytotoxic T cells.

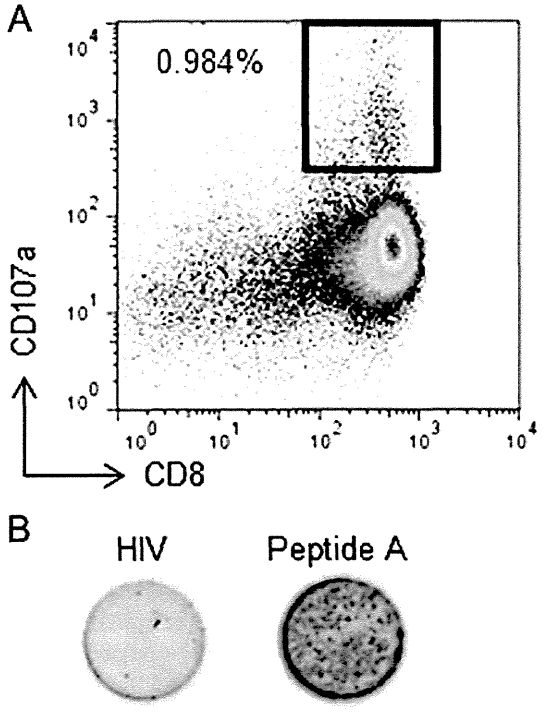

Figure 3. Peptide A-specific CTL clone established from anti-EML4-ALK CTL. (A) Peptide A-specific CTL clones established using CD107a single cell sorting. Peptide A-specific CTLs ($1x10^5$) were incubated with peptide-pulsed T2 cells ($5x10^4$) with CD107a-specific antibodies for 3.5 h at 37˚C. $CD8^+CD107a^+$ cells were sorted using a FACSAria II cell sorter. Square, $CD8^+CD107a^+$ cells that are peptide A-specific CTL clones. (B) Recognition of peptide-pulsed T2 cells by peptide A-specific CTL clones. A peptide A-specific CTL clone ($1x10^4$ cells) was incubated with stimulator cells that had been pulsed with 1 μM peptide A or HIV-gag peptide. IFN-γ-producing CTLs were detected by IFN-γ ELISPOT assay. CTLs, cytotoxic T cells.

peptide C), but peptide A was able to induce CTLs in three of four donors (healthy donors 2, 3 and 4). Based on this result, we used peptide A for further examinations.

Next, we obtained one CTL clone from peptide A-specific CTLs that was able to specifically recognize T2 cells pulsed with peptide A, but not T2 cells pulsed with an irrelevant HIV-gag peptide, using single cell sorting with a CD107a antibody. The population of $CD8^+CD107a^+$ cells represented 0.984% of all stimulated cells (Fig. 3A). These cells were sorted as single cells in each well of a 96-well plate. Twenty-one days after cell sorting, peptide specificity was assessed using the IFN-γ ELISPOT assay (Fig. 3B). The established clone reacted to the T2 cells pulsed with peptide A, but not to T2 cells pulsed with the irrelevant HIV-gag peptide. These results indicate that a peptide A-specific CTL clone was successfully established from PBMCs from a healthy donor.

*The EML4-ALK-specific CTL clone recognizes HLA-A*02:01$^+$ lung carcinoma cells with the EML4-ALK variant 3a/b incubated with IFN-γ.* We next evaluated the ability of the EML4-ALK-specific CTL clone to recognize the cancer cell line H2228, which expresses HLA-A*02:01 and EML4-ALK, using the IFN-γ ELISPOT assay. Even though the EML4-ALK-specific CTL clone failed to recognize H2228 cells, it did recognize those pretreated with 100 U/ml IFN-γ 48 h prior to examination (Fig. 4A). We examined the effect of IFN-γ on H2228 cells. Incubating target cells with IFN-γ for 48 h increased the expression of MHC class I molecules on the cell surface (Fig. 4B). This result indicates that the peptide A-specific CTL clone was able to recognize H2228 cells because of increased expression of MHC-class I on the H2228 cell surface.

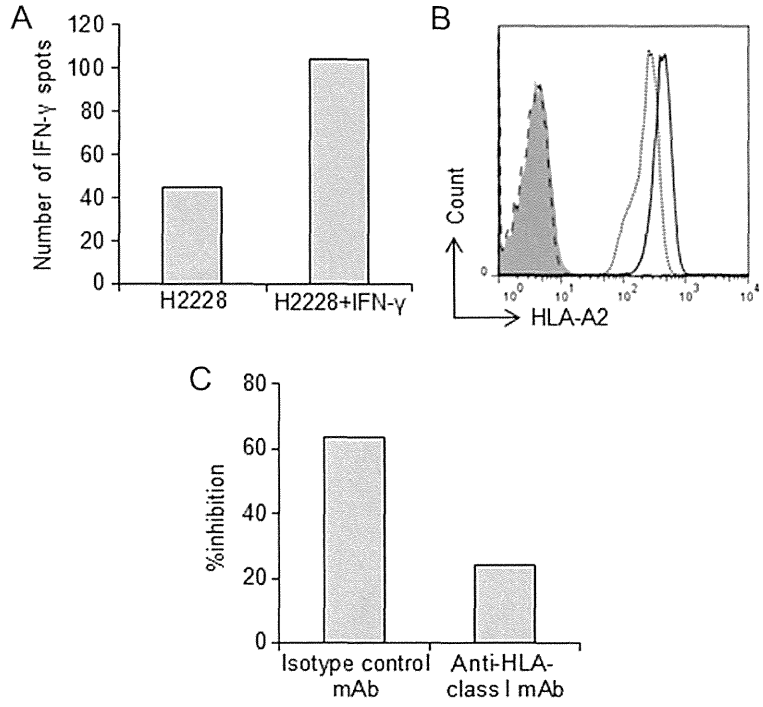

Figure 4. Recognition of lung carcinoma cells expressing HLA-A*02:01 and the EML4-ALK fusion gene by the peptide A-specific CTL clone. The peptide A-specific CTL clone recognized H2228 cells pretreated with IFN-γ 48 h prior to the assay. (A) The peptide A-specific CTL clone ($1x10^4$ cells) was incubated with H2228 cells with or without IFN-γ. IFN-γ production was detected by IFN-γ ELISPOT assay. (B) IFN-γ increased expression of HLA-A2 presented on H2228 cells. Incubation of H2228 cells with 100 U/ml IFN-γ for 48 h increased HLA-A2 presentation on the cells. Dotted line, HLA-A2 on H2228 cells without IFN-γ. Black line, HLA-A2 on H2228 cells incubated with IFN-γ (higher than on H2228 cells without IFN-γ). Dashed line and shaded region: no staining of H2228 cells with/without IFN-γ. (C) Inhibition of IFN-γ production by an anti-HLA-class I mAb. Blocking experiments were performed using an HLA-A, -B, -C-specific mAb (W6/32) or an isotype control mAb (mIgG2a,κ). The peptide A-specific CTL clone was incubated with H2228 cells (HLA-A*02:01+/EML4-ALK+) pretreated with IFN-γ 48 h prior to examination. IFN-γ-producing CTL clones were detected by IFN-γ ELISPOT assay. The bar graph shows the percentage of inhibition. CTL, cytotoxic T cell.

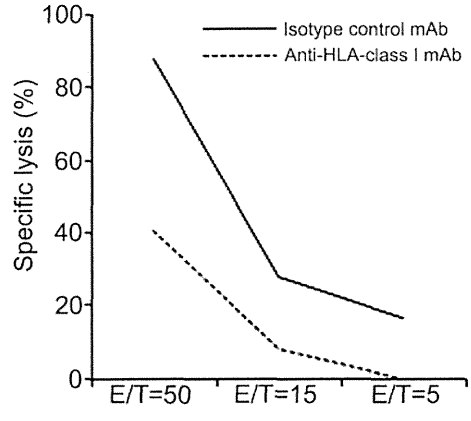

Figure 5. Cytotoxic activity of the peptide A-specific CTL clone against H2228 cells. The peptide A-specific CTL clone was incubated with H2228 cells pretreated with IFN-γ 48 h prior to the assay at various E/T ratios, and specific lysis was assessed. Blocking experiments were performed using the HLA-A, -B, -C-specific mAb (W6/32) or the isotype control mAb (mIgG2a,κ). CTL, cytotoxic T cell.

Specific IFN-γ production by the peptide A-specific CTL clone was detectable in H2228 cells treated with IFN-γ. The specificity was abolished by an anti-HLA-class I mAb, but not by an isotype control, suggesting that the observed production was HLA-A2 restricted (Fig. 4C).

A cytotoxicity assay was also performed. The peptide A-specific CTL clone was able to specifically lyse H2228 cells pretreated with IFN-γ 48 h prior to examination. This specific lysis was blocked by the anti-HLA-class I mAb, but not by the isotype control. These results indicate that the peptide A-specific CTL clone showed cytotoxicity and the ability to produce IFN-γ against HLA-A*02:01+ EML4-ALK+ NSCLC cell lines (Fig. 5).

Discussion

In the present study, we identified a new tumor-associated CTL epitope (peptide A) derived from EML4-ALK, which binds to HLA-A*02:01 molecules, and we were able to establish a peptide-specific CTL clone from human PBMCs that specifically recognized cognate peptide-pulsed T2 cells and HLA-A*02:01 tumor cells expressing EML4-ALK that had been pretreated with IFN-γ.

EML4-ALK-positive lung cancers are highly sensitive to ALK inhibition. However, as with trastuzumab or gefitinib (30,31), patients typically gain resistance within 1 to 2 years of starting therapy (23). We aimed to overcome these difficulties with immunotherapy.

We identified a glypican-3 (GPC3)-derived peptide and showed that GPC3-specific CTL frequency after vaccination correlated with OS. OS was significantly longer in patients with high GPC3-specific CTL frequencies than in those

with low frequencies (32). This indicates that the ability to induce a peptide-specific CTL clone is important for effective immunotherapy. We also revealed that GPC3 is an ideal target for anticancer immunotherapy since it is specifically overexpressed in hepatocellular carcinoma (HCC) (33-35).

In the present study, we chose a peptide array from EML4-ALK, from which we were able to induce a peptide-specific CTL clone. EML4-ALK is a strong oncogene overexpressed in cancer cells of NSCLC, breast cancer, kidney cancer and colon cancer (17). We performed RT-PCR and assayed the EML4 DNA levels of certain lung cancer cell lines. H2228 cells express EML4 moderately but at higher levels than other lung cancer cell lines. EML4 expression has been reported as highly expressed in $CD8^+$ T cells. RT-PCR showed that EML4 DNA levels were high in PBMCs and $CD8^+$ T cells. Because of a lack of suitable antibodies, we could not perform western blotting. However, our success at inducing a peptide A-specific CTL clone from $CD8^+$ T cells indicated that the CTL clone had no cytotoxicity against $CD8^+$ T cells.

This CTL clone could not recognize cancer cell lines without the ability to increase the amount of HLA class I presented on cell surfaces. Further examination is needed to achieve higher tumor reactivity. Combination chemotherapy or radiation therapy plus immunotherapy was recently reported to have a synergistic effect (36). Moreover, some mechanisms of synergy between radiation therapy, chemotherapy and immunotherapy have been revealed (37). In one of the mechanisms, these therapies upregulated tumor antigens and MHC moieties. These results suggest that combination therapy could be used to make tumor cell lines more susceptible to this peptide A-specific CTL clone-mediated cytolysis (38-41).

In addition, this treatment may be able to overcome resistance to ALK inhibition. Some resistance mechanisms for targeting drugs have been examined. The most commonly identified causes of resistance are point mutations such as L1196M (42-44), G1269A (22) and S1206Y (21). These point mutations occur in the tyrosine kinase domain, which plays an important role in oncogenesis. Our peptide array was selected from EML4, which has no correlation with these point mutations. It is possible that this treatment is effective for tumor cells resistant to ALK inhibitors.

In this study, we identified a new epitope peptide derived from the EML4-ALK fusion gene. We successfully induced an HLA-A*02:01-restricted peptide-specific CTL clone that demonstrated cytotoxicity for EML4-ALK-positive tumor cells. This is a new epitope-based vaccine therapy design for EML4-ALK-positive cancer cells. In order to obtain a stronger effect, further analysis is needed.

Acknowledgements

We thank Professor S. Yano for providing the H2228 cell line, which possesses the EML4-ALK fusion gene, Professor H. Mano for providing the EML4-ALK fusion DNA and Professor N. Hirano for providing artificial APCs. This study was supported in part by Health and Labor Science Research Grants for Clinical Research and Third Term Comprehensive Control Research for Cancer from the Ministry of Health, Labor and Welfare, Japan and the National Cancer Center Research and Development Fund (25-A-7).

References

1. Silvestri GA, Tanoue LT, Margolis ML, *et al*: The noninvasive staging of non-small cell lung cancer: the guidelines. Chest 123: 147S-156S, 2003.
2. Reck M: What future opportunities may immuno-oncology provide for improving the treatment of patients with lung cancer? Ann Oncol 23 (Suppl 8): viii28-viii34, 2012.
3. Chang SC, Chang CY and Shih JY: The role of epidermal growth factor receptor mutations and epidermal growth factor receptor-tyrosine kinase inhibitors in the treatment of lung cancer. Cancers 3: 2667-2678, 2011.
4. Gridelli C, Peters S, Sgambato A, Casaluce F, Adjei AA and Ciardiello F: ALK inhibitors in the treatment of advanced NSCLC. Cancer Treat Rev 40: 300-306, 2014.
5. Hall RD, Gray JE and Chiappori AA: Beyond the standard of care: a review of novel immunotherapy trials for the treatment of lung cancer. Cancer Control 20: 22-31, 2013.
6. Jackman DM, Miller VA, Cioffredi LA, *et al*: Impact of epidermal growth factor receptor and KRAS mutations on clinical outcomes in previously untreated non-small cell lung cancer patients: results of an online tumor registry of clinical trials. Clin Cancer Res 15: 5267-5273, 2009.
7. West H, Oxnard GR and Doebele RC: Acquired resistance to targeted therapies in advanced non-small cell lung cancer: new strategies and new agents. Am Soc Clin Oncol Educ Book, 2013. doi: 10.1200/EdBook_AM.2013.33.e272. (http://meetinglibrary.asco.org/content/198-132).
8. Wu YL, Park K, Soo RA, *et al*: INSPIRE: a phase III study of the BLP25 liposome vaccine (L-BLP25) in Asian patients with unresectable stage III non-small cell lung cancer. BMC Cancer 11: 430, 2011.
9. Tyagi P and Mirakhur B: MAGRIT: the largest-ever phase III lung cancer trial aims to establish a novel tumor-specific approach to therapy. Clin Lung Cancer 10: 371-374, 2009.
10. Quoix E, Ramlau R, Westeel V, *et al*: Therapeutic vaccination with TG4010 and first-line chemotherapy in advanced non-small-cell lung cancer: a controlled phase 2B trial. Lancet Oncol 12: 1125-1133, 2011.
11. Brahmer JR, Tykodi SS, Chow LQ, *et al*: Safety and activity of anti-PD-L1 antibody in patients with advanced cancer. N Engl J Med 366: 2455-2465, 2012.
12. Lynch TJ, Bondarenko I, Luft A, *et al*: Ipilimumab in combination with paclitaxel and carboplatin as first-line treatment in stage IIIB/IV non-small-cell lung cancer: results from a randomized, double-blind, multicenter phase II study. J Clin Oncol 30: 2046-2054, 2012.
13. Topalian SL, Hodi FS, Brahmer JR, *et al*: Safety, activity, and immune correlates of anti-PD-1 antibody in cancer. N Engl J Med 366: 2443-2454, 2012.
14. Soda M, Choi YL, Mano H, *et al*: Identification of the transforming EML4-ALK fusion gene in non-small-cell lung cancer. Nature 448: 561-566, 2007.
15. Bonanno L, Favaretto A, Rugge M, *et al*: Role of genotyping in non-small cell lung cancer treatment: current status. Drugs 71: 2231-2246, 2011.
16. Fukui T, Yatabe Y, Mitsudomi T, *et al*: Clinicoradiologic characteristics of patients with lung adenocarcinoma harboring EML4-ALK fusion oncogene. Lung Cancer 77: 319-325, 2012.
17. Lin E, Li L, Guan Y, *et al*: Exon array profiling detects EML4-ALK fusion in breast, colorectal, and non-small cell lung cancers. Mol Cancer Res 7: 1466-1476, 2009.
18. Robertson FM, Petricoin Iii EF, Cristofanilli M, *et al*: Presence of anaplastic lymphoma kinase in inflammatory breast cancer. Springerplus 2: 497, 2013.
19. Sasaki T, Rodig SJ, Jänne PA, *et al*: The biology and treatment of EML4-ALK non-small cell lung cancer. Eur J Cancer 46: 1773-1780, 2010.
20. Kwak EL, Bang YJ, Iafrate AJ, *et al*: Anaplastic lymphoma kinase inhibition in non-small-cell lung cancer. New Engl J Med 363: 1693-1703, 2010.
21. Katayama R, Shaw AT, Engelman JA, *et al*: Mechanisms of acquired crizotinib resistance in ALK-rearranged lung cancers. Sci Transl Med 4: 120ra17, 2012.
22. Doebele RC, Pilling AB, Camidge DR, *et al*: Mechanisms of resistance to crizotinib in patients with ALK gene rearranged non-small cell lung cancer. Clin Cancer Res 18: 1472-1482, 2012.
23. Shaw AT and Engelman JA: ALK in lung cancer: past, present, and future. J Clin Oncol 31: 1105-1111, 2013.

24. Sasaki T, Koivunen J, Jänne PA, *et al*: A novel ALK secondary mutation and EGFR signaling cause resistance to ALK kinase inhibitors. Cancer Res 71: 6051-6060, 2011.
25. Latif M, Saeed A and Kim SH: Journey of the ALK-inhibitor CH5424802 to phase II clinical trial. Arch Pharm Res 36: 1051-1054, 2013.
26. Passoni L, Scardino A, Gambacorti-Passerini C, *et al*: ALK as a novel lymphoma-associated tumor antigen: identification of 2 HLA-A2.1-restricted CD8$^+$ T-cell epitopes. Blood 99: 2100-2106, 2002.
27. Hirohashi Y, Torigoe T, Maeda A, *et al*: An HLA-A24-restricted cytotoxic T lymphocyte epitope of a tumor-associated protein, survivin. Clin Cancer Res 8: 1731-1739, 2002.
28. Hirano N, Butler MO, Xia Z, *et al*: Engagement of CD83 ligand induces prolonged expansion of CD8$^+$ T cells and preferential enrichment for antigen specificity. Blood 107: 1528-1536, 2006.
29. Yoshikawa T, Nakatsugawa M, Sakemura N, *et al*: HLA-A2-restricted glypican-3 peptide-specific CTL clones induced by peptide vaccine show high avidity and antigen-specific killing activity against tumor cells. Cancer Sci 102: 918-925, 2011.
30. Robinson KW and Sandler AB: EGFR tyrosine kinase inhibitors: difference in efficacy and resistance. Curr Oncol Rep 15: 396-404, 2013.
31. Lesniak D, Sabri S, Abdulkarim B, *et al*: Spontaneous epithelial-mesenchymal transition and resistance to HER-2-targeted therapies in HER-2-positive luminal breast cancer. PLoS One 8: e71987, 2013.
32. Sawada Y, Yoshikawa T, Nakatsura T, *et al*: Phase I trial of a glypican-3-derived peptide vaccine for advanced hepatocellular carcinoma: immunologic evidence and potential for improving overall survival. Clin Cancer Res 18: 3686-3696, 2012.
33. Nakatsura T, Yoshitake Y, Nishimura Y, *et al*: Glypican-3, over-expressed specifically in human hepatocellular carcinoma, is a novel tumor marker. Biochem Biophys Res Commun 306: 16-25, 2003.
34. Okabe H, Satoh S, Nakamura Y, *et al*: Genome-wide analysis of gene expression in human hepatocellular carcinomas using cDNA microarray: identification of genes involved in viral carcinogenesis and tumor progression. Cancer Res 61: 2129-2137, 2001.
35. Saito-Hisaminato A, Katagiri T, Nakamura Y, *et al*: Genome-wide profiling of gene expression in 29 normal human tissues with a cDNA microarray. DNA Res 9: 35-45, 2002.
36. Weir GM, Liwski RS and Mansour M: Immune modulation by chemotherapy or immunotherapy to enhance cancer vaccines. Cancers 3: 3114-3142, 2011.
37. Hodge JW, Ardiani A, Gameiro SR, *et al*: The tipping point for combination therapy: cancer vaccines with radiation, chemotherapy, or targeted small molecule inhibitors. Semin Oncol 39: 323-339, 2012.
38. Garnett CT, Palena C, Hodge JW, *et al*: Sublethal irradiation of human tumor cells modulates phenotype resulting in enhanced killing by cytotoxic T lymphocytes. Cancer Res 64: 7985-7994, 2004.
39. Gelbard A, Garnett CT, Hodge JW, *et al*: Combination chemotherapy and radiation of human squamous cell carcinoma of the head and neck augments CTL-mediated lysis. Clin Cancer Res 12: 1897-1905, 2006.
40. Kaneno R, Shurin GV, Shurin MR, *et al*: Chemotherapeutic agents in low noncytotoxic concentrations increase immunogenicity of human colon cancer cells. Cell Oncol 34: 97-106, 2011.
41. Ramakrishnan R, Assudani D, Gabrilovich DI, *et al*: Chemotherapy enhances tumor cell susceptibility to CTL-mediated killing during cancer immunotherapy in mice. J Clin Invest 120: 1111-1124, 2010.
42. Choi YL, Soda M, Yamashita Y, *et al*: EML4-ALK mutations in lung cancer that confer resistance to ALK inhibitors. N Engl J Med 363: 1734-1739, 2010.
43. Katayama R, Khan TM, Benes C, *et al*: Therapeutic strategies to overcome crizotinib resistance in non-small cell lung cancers harboring the fusion oncogene EML4-ALK. Proc Natl Acad Sci USA 108: 7535-7540, 2011.
44. Lovly CM and Pao W: Escaping ALK inhibition: mechanisms of and strategies to overcome resistance. Sci Transl Med 4: 120ps2, 2012.

Journal of Hepatocellular Carcinoma

Dovepress

open access to scientific and medical research

Open Access Full Text Article

REVIEW

Critical analysis of the potential of targeting GPC3 in hepatocellular carcinoma

This article was published in the following Dove Press journal:
Journal of Hepatocellular Carcinoma
21 May 2014
Number of times this article has been viewed

Kazuya Ofuji
Keigo Saito
Toshiaki Yoshikawa
Tetsuya Nakatsura

Division of Cancer Immunotherapy, Exploratory Oncology Research and Clinical Trial Center, National Cancer Center, Kashiwa, Japan

Abstract: Hepatocellular carcinoma (HCC) is a leading cause of cancer-related deaths worldwide. The treatment options for patients with advanced HCC are limited, and novel treatment strategies are required urgently. Glypican-3 (GPC3), a member of the glypican family of heparan sulfate proteoglycans, is overexpressed in 72%–81% of HCC cases, and is correlated with a poor prognosis. GPC3 regulates both stimulatory and inhibitory signals, and plays a key role in regulating cancer cell growth. GPC3 is released into the serum, and so might be a useful diagnostic marker for HCC. GPC3 is also used as an immunotherapeutic target in HCC. A Phase I study of a humanized anti-GPC3 monoclonal antibody, GC33, revealed a good safety profile and potential antitumor activity, and a Phase II trial is currently ongoing. In addition, the authors' investigator-initiated Phase I study of a GPC3-derived peptide vaccine showed good safety and tolerability, and demonstrated that the GPC3 peptide-specific cytotoxic T-lymphocyte frequency in peripheral blood correlated with overall survival in HCC patients. A sponsor-initiated Phase I clinical trial of a three-peptide cocktail vaccine, which includes a GPC3-derived peptide, is also underway. GPC3 is currently recognized as a promising therapeutic target and diagnostic marker for HCC. This review introduces the recent progress in GPC3 research, from biology to clinical impact.

Keywords: GPC3, hepatocellular carcinoma, immunotherapy

Introduction

Hepatocellular carcinoma (HCC) is the third leading cause of cancer-related deaths worldwide.[1] HCC patients are often diagnosed at an advanced stage, and so the prognosis is often poor. Currently, surgery or locally ablative treatments such as percutaneous ethanol injection or radiofrequency ablation are the standard treatments for early-stage HCC. However, these treatments are no longer available and options are limited for most patients with advanced HCC.[2] Generally, transarterial chemoembolization or systemic chemotherapy is used. However, these therapeutic approaches are not curative in most patients. Sorafenib, a multi-targeted tyrosine kinase inhibitor, is the only drug that has significantly prolonged the survival of patients with advanced HCC;[3,4] therefore, it has become the standard agent for first-line systemic treatment. However, the incidence of adverse effects is high, and there are no effective second-line treatments for patients who do not respond to sorafenib. Therefore, new treatment strategies for patients with advanced HCC should be established.

To date, several immunotherapeutic clinical trials in patients with advanced HCC have been performed. These studies have shown feasibility and safety, but no dramatic clinical responses.[5,6] Nevertheless, some randomized controlled trials have shown the

Correspondence: Tetsuya Nakatsura
Division of Cancer Immunotherapy, Exploratory Oncology Research and Clinical Trial Center, National Cancer Center, 6-5-1 Kashiwanoha, Kashiwa 277-8577, Japan
Tel +81 4 7131 5490
Fax +81 4 7133 6606
Email tnakatsu@east.ncc.go.jp

submit your manuscript | www.dovepress.com
Dovepress
http://dx.doi.org/10.2147/JHC.S48517

potential to reduce the risk of cancer recurrence in adjuvant settings.[6] Therefore, an immunotherapeutic approach is potentially an attractive treatment option for HCC.

Various tumor antigens for HCC have been identified and investigated as immunotherapeutic targets.[7] GPC3 is a member of the glypican family of heparan sulfate proteoglycans that are attached to the cell surface via glycosylphosphatidylinositol (GPI) anchors.[8] Mutations in *GPC3* cause Simpson–Golabi–Behmel syndrome,[9] which is an X-linked disorder characterized by pre- and postnatal overgrowth with visceral and skeletal anomalies. *GPC3*-deficient mice exhibited similar characteristics as Simpson–Golabi–Behmel syndrome patients.[10] GPC3 is overexpressed in 72%–81% of patients with HCC.[11–15] Therefore, GPC3 has been recognized as a potential immunotherapeutic target or diagnostic marker for HCC. This paper reviews the biology of GPC3 and discusses recent advances in GPC3-targeted HCC immunotherapy.

Tumor-associated antigens (TAAs) in HCC

TAA-specific immunotherapy is an attractive strategy because it is associated with fewer adverse events. Therefore, identifying appropriate TAAs is important for the development of TAA-specific cancer immunotherapies. Boon et al initially reported that MAGE-A was a human TAA in a melanoma patient, and that the human immune system could recognize TAA expressing-cancer cells as foreign bodies and exclude them.[16] Subsequently, a novel approach termed serological analysis of recombinant complementary DNA expression libraries (SEREX) was developed to identify TAAs.[17,18] Complementary DNA microarray technology is also useful for identifying novel cancer-associated genes and for classifying human cancers at the molecular level.[19,20] In HCC, some TAAs, such as AFP, MAGE-A, NY-ESO-1, SSX2, and telomerase reverse transcriptase, have been identified.[7] Although GPC3 is overexpressed in HCC,[11–15] it is not expressed in most normal adult tissues. Furthermore, GPC3-expression was correlated with poor prognosis in patients with HCC: GPC3-positive HCC patients had a significantly lower 5-year survival rate than GPC3-negative individuals (54.5% versus 87.7%; P=0.031).[15] These results suggest that GPC3 might be a promising target for cancer immunotherapy.

Biological aspects of GPC3

General considerations

Glypicans are a family of heparan sulfate proteoglycans. To date, six glypicans have been identified (GPC1 to GPC6) in mammals, and two orthologs of the mammalian genes were identified in *Drosophila melanogaster* (Dally- and Dally-like).[8,21] Glypicans of all species are classified into two subfamilies according to their sequence homology.[21] In general, the function of glypicans is to regulate morphogenesis during embryonic development,[22] and mutations cause the overgrowth genetic disease Simpson–Golabi–Behmel syndrome.[23] Several recent studies have revealed that GPC3 is overexpressed in many cancers.

Structure and function of GPC3

GPC3 is a 580-amino acid protein (~60 kDa) that is encoded by nine exons on chromosome X (Xq26). Alternative splicing results in four variants that were isolated from the HepG2 cell line. Fourteen cysteine residues located in the core region are well conserved among glypicans, and contribute to the formation of a unique ternary structure via disulfide bonds. The amino-terminus contains a signal peptide sequence (residues 1–24), which is required for targeting to the cell surface. The carboxyl-terminus contains a hydrophobic region that is associated with the lipid bilayer of the Golgi apparatus. During the transport of GPC3 to the cell surface, the hydrophobic region is truncated by transamidase, and then covalently attached to a GPI anchor via the C-terminus of serine 560.[24] Therefore, the attachment of a GPI anchor is a key post-translational modification that regulates the cellular localization of GPC3.

GPC3 regulates both stimulatory and inhibitory signals through the binding of heparan sulfate chains to signaling molecules such as Wnt, Hedgehog, fibroblast growth factors, bone morphogenetic proteins.[25–31] The core protein also plays an important role for regulating the activity in Wnt and Hedgehog signaling.[27,28,32] Structural information regarding GPC3 is needed to understand these signaling mechanisms, but the three-dimensional structure of GPC3 is yet to be elucidated. Nevertheless, the crystal structure of *Drosophila* Dlp, an ortholog of the mammalian gene, is available.[33] Structural analysis of the Dlp core region revealed an elongated conformation with α-helix packing: this is a unique structure when compared with other proteins. Further structural studies of glypicans are necessary to understand their complex and multifunctional signaling pathways and their regulation of cancer cell growth.

GPC3 biology and disease

GPC3 is expressed in many embryonic tissues in addition to fetal liver and placenta.[34] The overexpression of GPC3 is observed in liver cancer, ovarian cancer, lung cancer, malig-

nant melanoma, and embryonal cancers such as neuroblastoma medulloblastoma and Wilms' tumor.[35–41] Capurro et al demonstrated that the binding of GPC3 to Wnt and Hedgehog activates signaling pathways that promote the growth of HCC cells.[27,28] Moreover, the knockdown of GPC3 using small interfering RNA and subsequent gene expression analysis revealed that suppressing GPC3 inhibited the transforming growth factor-β (TGF-β) receptor pathway and the subsequent growth of HCC cell lines.[42] These suggest that GPC3 is an important target for cancer therapy.[43,44]

It is noteworthy that GPC is a novel serological cancer marker.[12,45,46] Secreted circulating GPC3 is detected in the blood of cancer patients with HCC[11,45] and melanoma,[37,47]and the presence of soluble GPC3 correlates with cancer progression. However, because GPC3 is initially membrane-bound via a GPI anchor, it is currently unknown how GPC3 is secreted into the circulation. It was reported that GPC3 can be cleaved by Notum (α/β-hydrolase enzyme) and furin-like convertase,[48,49] releasing the N-terminal domain and full-length GPC3 from the cell surface.[50,51] Secreted GPC3 might be useful for cancer diagnosis.

GPC3 as a diagnostic marker for HCC

GPC3 expression in HCC at the messenger RNA or protein level

Several studies have suggested that GPC3 is a potential therapeutic target in liver cancer because it is overexpressed in HCC, but is not expressed or is expressed at only low levels in normal adult tissue.[52–54] Hsu et al performed pioneering work to identify GPC3 as a potential biomarker for HCC.[55] When GPC3 was compared with AFP, another established HCC marker, data revealed higher *GPC3* messenger RNA expression compared with serum α-fetoprotein (AFP), levels (71.7% versus 51.3%) based on the analysis of 113 patients with unicentric primary HCC. The authors also reported previously that *GPC3* is specifically overexpressed in HCC by analyzing complementary DNA microarrays containing 23,040 genes. The expression profiles of 20 HCC samples, corresponding noncancerous liver tissues, and various normal human tissues revealed that GPC3 was overexpressed specifically in HCC.[11]

Capurro et al confirmed increased GPC3 expression in HCC patients using a mouse monoclonal antibody (1G12) against a GPC3 C-terminal peptide.[12] Immunohistochemistry revealed that GPC3 was overexpressed in 72% of HCC samples. Therefore, GPC3 might also be useful as an ancillary tool during histopathological diagnostic processes to distinguish HCC from cirrhosis, dysplastic nodules, and focal nodular hyperplasia-like nodules.[56]

GPC3 as a serum marker for HCC

Several studies have been performed to validate the diagnostic potential of GPC3 as a serum marker by developing methodologies such as enzyme-linked immunosorbent assays and radioimmunoassays.[45,57] Several antibody-based immunoassays have been developed to assess potential serum biomarkers. Using multiple serum markers, including AFP and protein induced by vitamin K absence or antagonists-II (PIVKA-II), might increase diagnostic accuracy. Although GPC3 is a cell-surface marker, it can be released into the serum by the lipase Notum, which cleaves the GPI anchor.[49] Specifically, Hippo et al reported that GPC3 is cleaved between Arg358 and Ser359, and that the N-terminal fragment of GPC3 is also released into circulation. They reported the usefulness of the N-terminal fragment of GPC3 for diagnosing early-stage HCC.[51] Therefore, GPC3 also exhibits diagnostic value as a serum marker.[57,58] Qiao et al compared the serum levels of three markers (GPC3, human cervical cancer oncogene [HCCR], and AFP) for diagnosing HCC in 189 patients (101 HCC, 40 cirrhosis, and 18 hepatitis cases and 30 healthy control donors). They reported that GPC3 was the most accurate diagnostic marker: using a cutoff of 26.8 ng/mL for the diagnosis of HCC, GPC3 had a sensitivity of 51.5% and a specificity of 92.8%. In addition, the simultaneous detection of three markers increased the sensitivity significantly to 80.2% higher than AFP alone.[58] In a meta-analysis comparing AFP and GPC3 as serum markers for HCC, the pooled sensitivities for AFP and GPC3 were 51.9% and 59.2%, and the pooled specificities were 94% and 84.8%, respectively.[59] This suggests that GPC3 and AFP are comparable serum markers. Serum GPC3 might be a useful tumor marker in patients with HCC. However, the biochemistry of serum GPC3 is yet to be elucidated, and so further studies are needed.

GPC3 as an immunotherapeutic target in HCC

Identification of human leukocyte antigen (HLA)-A2- or A24-restricted GPC3-derived epitope peptides

Identifying TAA-derived epitope peptides is the first step in the development of peptide vaccines. *HLA-A24* is the most common HLA class I allele in the Japanese population (60%).[60,61] Structural motifs of peptides bound to human HLA-A24 and BALB/c mouse H-2K^d are similar,[62,63] and the amino acid sequences of human and mouse GPC3 have 95% homology. These studies identified the mouse GPC3-derived